Sound Absorptivity of Various Designs of 3-D Printed Acoustic Paneling

by

Nathan Davis

Submitted in Partial Fulfillment of the Requirements

for the Degree of

Master of Science in Engineering

in the

Electrical Engineering

Program

YOUNGSTOWN STATE UNIVERSITY

May 2021

Sound Absorptivity of Various Designs of 3-D Printed Acoustic Paneling

Nathan Davis

I hereby release this Thesis to the public. I understand that Thesis will be made available from the OhioLINK ETD Center and the Maag Library Circulation Desk for public access. I also authorize the University or other individuals to make copies of this thesis as needed for scholarly research.

Signature:

_____

Nathan Davis, Student Date

Approvals:

_____

Dr. Eric MacDonald, Thesis Advisor Date

_____

Dr. Anindita Paul, Committee Member Date

_____

Dr. Pedro Cortes, Committee Member Date

_____

Dr. Salvatore A. Sanders, Dean of Graduate Studies Date

Abstract

As the world population grows into a more urbanized state, the concern for noise pollution continues to grow with it. Noise pollution has been shown to be a source of several negative health consequences, including ill impacts on cardiovascular health, mental health and sleep hygiene. Some solutions are able to effectively reduce noise pollution. One example is highway noise barriers that reduce traffic noise to a bearable level for residential areas located near the highway. These sound barriers, however, not only cost a lot of money and require a significant amount of resources, but structural limitations and the ever growing noise floor will eventually cause these barriers to be obsolete. This study aims to evaluate the design of 3D printed sound absorbing acoustic panels that could augment if not replace current acoustical treatments. In so doing, four different designs of sound panels were 3D printed and tested for their effectiveness in reducing reverberation time and sound amplitude in a controlled environment. It was found that all four of the designs printed in this study notably reduce reverberation time by up to 12.7%, three of which also significantly reduced the amplitude of the sound by up to 5 dB. The aforementioned designs thus can serve as a useful adjunct to reducing sound pollution and all the ill effects caused by it, along with the added benefit of employing the accessibility of 3D printing along with its lower-cost materials.

Table of Contents

Chapter 1 – Introduction

Noise pollution poses a threat to public health and is prevalent in almost any urban area. Noise can be defined as any sounds that are unwanted. The noise pollution levels are projected to continue to increase which can be accredited to the continuous growth of population and urbanization. Cars, airplanes, trains, factories among others are some of the main culprits that are contributing to the ever-increasing levels of noise pollution. A study by Jariwala et al. states that noise pollution can have several adverse effects on health [1]. Hearing impairment can occur as a direct result from noise pollution which can immediately diminish one's well-being and safety. Additionally, if there is extended exposure to sound pressure levels above 85 decibels (dB) it can result in permanent hearing loss. Hearing impairment is not the only health threat posed by noise pollution. Noise pollution has also been shown to have negative effects on cardiovascular health, mental health, and sleep hygiene. Being woken up from a loud noise is probably one of the most obvious setbacks from noise pollution [2]. Disruptions in the sleep cycle can result in mood changes, decrease in overall performance, as well as other negative underlying health effects. Loud noises can act as stressors that trigger the body's sympathetic nervous system (fight or flight response) which temporarily increases a person's blood pressure, heart rate, and cause vasoconstriction [2]. While temporary noise exposure has reversible cardiovascular effects, chronic exposure to loud noises is correlated with more permanent cardiovascular disease. Noise pollution is not a suggested as a direct cause of any mental illnesses but is assumed to accelerate the development of some existing mental illnesses through an increase in anxiety, headache, stress, emotional instability, etc. Prolonged

exposure to noise levels above 80 dBA (dBA = dB A-weighted which is a measurement that corresponds to how humans hear), which is the noise level as a power lawnmower or heavy traffic, are also linked to an increase in aggressive behavior towards others which is a common trend exhibited by news media covering stories of violent disputes over noise complaints [3]. In response to the adverse health effects caused by noise pollution, many attempts to reduce or block noise levels can be seen through structural and architectural design.

One such solution may be noticed while driving on the highway in the form of large, ornamental, acoustically treated walls. These walls act as noise barriers designed to address the roadway noise pollution issue and absorb a large portion of the sound made from cars on the highway. A study claims that highway sound barriers are able to reduce noise levels by approximately 11 dBA [4]. These walls are typically made up of porous concrete and steel and require significant resources such as workers, machinery, and fabrication materials to install along the highway [5],[6]. Since April of 2006, the U.S. has spent over $2.3 billion dollars on highway noise barriers[7] and the expenditure for these noise barriers continues to increase. With the heightened cost of noise barriers on our highways, a cheaper, more effective alternative is desirable. The alternatives proposed in this study employ the use of several lower-cost, 3D-printed structures that act as sound absorbers and could be used to reduce noise pollution.

This study will examine some of the existing innovative designs and methods that have been used to aid in the dissipation of unwanted noise as well as examine some of the methods that are used to test the effectiveness of said designs and methods. In an attempt to explore more options, this study proposed four new 3D-printable designs and tested the

effectiveness of the presented designs. One of these designs features elements of parabolic dishes which are typically used to focus light or sound. Another design looks into a newer concept known as phononic crystals that utilize structures that encourage passive destructive interference. The last two panels presented in this study are similar to each other and were inspired by the idea of trapping incoming sound waves with an array "arrow-like" structures.

The purpose of this study is to document the fabrication of cost-effective, 3D-printed acoustic paneling of various structural configurations, and evaluate their efficacy in absorbing noise of audible frequencies. These designs could be used for both for residential and commercial use. Such products would also have potential use in the field of public health, reducing noise pollution, as well as in industries and urban lifestyles where noise pollution poses an issue.

Chapter 2 - Literature Review

A 2014 acoustical study develops a method in dissipating low frequency sounds by using "dark" acoustic metamaterials as super absorbers. This study utilizes elastic silicone rubber in conjunction with a pattern of rigid platelets to achieve near unity absorption (~0.99 absorption coefficient) of low frequency sounds (<1000 Hz) . The elastic silicone catches the incoming sound waves as the platelets dampen the vibrations by adding resistance to the attenuation of the silicone. Testing for this study was conducted with a modified impedance tube apparatus to determine absorptive properties of developed metamaterials. This study concluded that the developed metamaterial may have applications in dissipating low frequency noise from large machinery and roadways [8].

A study conducted by Liu et al. tests feasibility of micro-perforated panels fabricated using 3D printing technology as acoustic absorbers and the effect they have on the sound absorption coefficient (SAC). This experiment used multiple different panels with different spacing of perforations. Each panel in this study had an absorption coefficient measured with a 2 microphone impedance tube configuration. The results of the impedance tube showed a relationship between the number of perforations that a panel has and the absorption peak location. The absorption peak for a panel with smallest perforation spacing was at the highest frequency compared to the panels with larger spaced perforations and the frequency absorption peak decreased proportionally as the spacing increased. This study concluded that this method could be a useful approach when trying to tune the absorption peaks of an area [9].

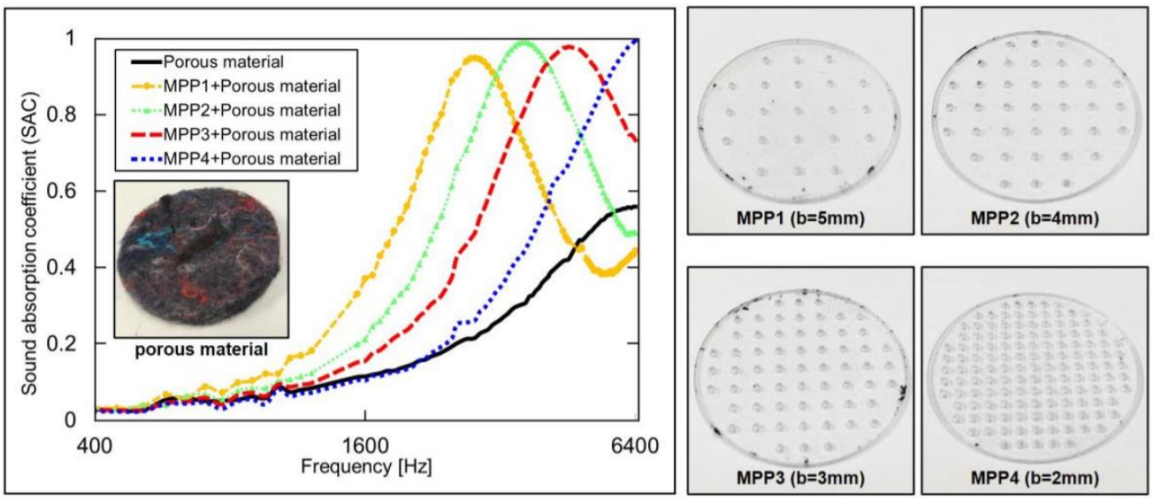

Figure 1: Effect of perforation ratio of the SAC for an MPP layer with porous material
Image Adapted from study by Liu et al. [9]

A physics textbook study aims to combat noise pollution and offer a better alternative to existing sound absorbers by introducing a 3D-printed lattice structure. This study focused on analyzing the effects the thickness of the material and the diameter of the lattice struts play on the absorption coefficient. The materials were measured using an

impedance tube configuration to determine the absorption coefficients of each material. It was determined from this study that the thickness of the used material does not have a great relationship with the absorption coefficient, but does impact absorption peak frequency: the thicker the material, the lower frequency of the absorption peak. However, the larger the diameter of the lattice strut, the higher the peak of absorption. This experiment used frequencies within 1.5 kHz and 2kHz. This study concluded that the presented lattice structure could be valuable in upcoming sound absorbing materials [10].

Figure 2: 3D-printed Lattice Structures with Varying Thickness
Image adapted from *Proceedings of Mechanical Engineering Research Day 2019* [10]

Another study from the same physics textbook tests the effectiveness of non-synthetic materials such as banana stem, grass, palm and palm oil leaves, as sound absorbing materials. This study argues that the use of these materials has a much less harmful effect on the health of humans and the environment. Each of the materials were pressed into small disks and subjected to an impedance tube configuration to obtain the absorption coefficients of each material. The experiment used frequencies between 0.1 kHz and 5 kHz. The study concluded that of the materials that were tested, palm leaves had the best results as an absorbing material. They also concluded that some of the used materials show good promise in becoming eco-friendly and possibly even better alternatives to synthetic materials [11].

Arjunan conducts a study that takes the approach of using geometry-controlled waveguides as a passive sound cancelling structure. The study discusses the possible use of proposed design in acoustic paneling. The idea of the design is to have sound waves

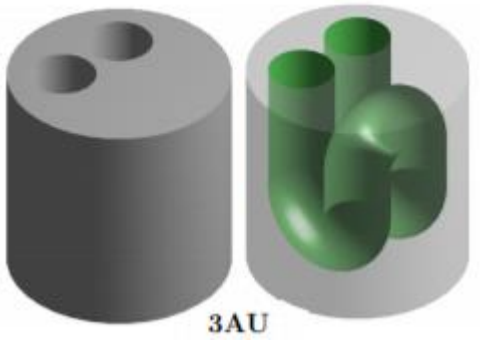

Figure 3: Complex Geometrical Waveguide Example
Image adapted from a study by Arjunan et al. [12]

enter from two opposite ends of a wave guide so that the split waves collide in opposite phases to create destructive interference and dissipate the majority of the wave. The study utilized 3D printing to create complex geometrical waveguides that fit into compact structures. Study discussed that depending on the geometry of the waveguide, it could be possible to target specific frequencies for dissipation via destructive interference cancelling. This could be a good option for addressing troublesome frequencies that other sound absorbing designs struggle in absorbing [12].

A study conducted in 2016 investigates the use of 3D printed flexible membrane-type acoustic metamaterial (MAM) as a method for absorbing lower, troublesome frequencies. In the presented experiment, a flexible disk is fabricated that has masses placed on the sample to provide resistance for applied soundwaves. An impedance tube was used to measure the absorption coefficients. The study claims that it could also be possible to fine tune the MAM absorber to specific frequencies based on the thickness of the disk and the geometry of the masses placed. This study claims that with the correct placement amount and placement of masses, that this could be a feasible option in mitigating broadband low frequency noise [13].

Figure 4: Printed Sample of MAM with Attached Mass
Image adapted from a study by Lavie et al. [13]

A journal study investigates using a series of microperforated panels (MPPs) in conjunction as a method for creating a wideband noise absorber. Each of the three different layers used in the triple layer MPP has its own diameter, thickness, perforation ratio, and air layer thickness. By optimizing via simulated annealing, the combination of the 4 components between the 3 layers, it is possible to get a wideband absorbing sample with a high with near unity absorption. This study claims that with the advancing technology that this could be a feasible method for controlling noise that exceeds the current technology [14].

Yang et al. aims to tackle noise pollution by employing 3D printed MPPs that have tunable wideband absorption. The study claims that by using 3D printing technology, it is possible to obtain geometrical shapes that are unobtainable by conventional subtractive manufacturing. Study claims that multi layered 3D printed samples that were fabricated not only cover a wider band of frequencies but also have comparable if not better absorption coefficients than those of conventional single-layered MPPs. Experiment included multiple different samples and varying the number of layers used as well as the distance between each of the MPPs. The experiment in this study concluded that the best coverage was obtained from using 3 layers of MPPs, especially with lower frequencies.

Study claims that 3D printing MPPs is an effective method to create tunable wideband absorbers that can be used in future technology to fight noise pollution [15].

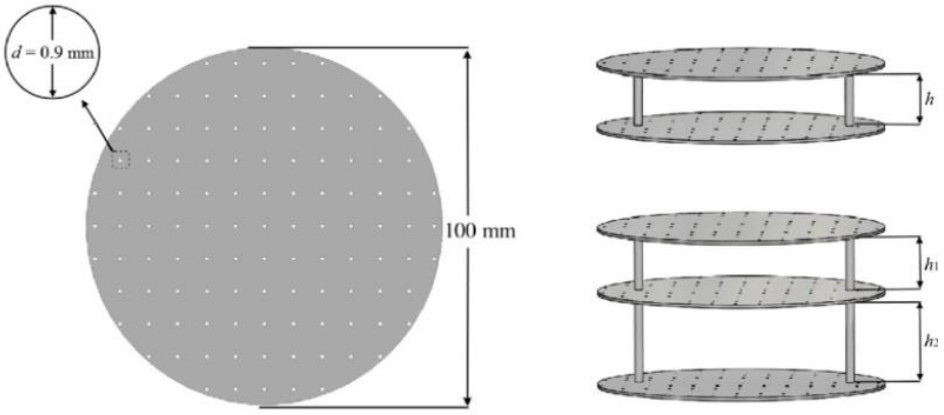

Figure 5: Single, Double, and Triple Layer MPP Samples
Image Adapted from a study by Yang et al. [15]

A NASA technical report explains the process in developing a way to suppress loud noises from aircraft engines in order to meet regulated noise levels. Study comes up with several different designs each suited for a specific need. This study concluded that in order to test the developed panels, it is sufficient to take a small section of the duct with a single microphone in each chamber within a lab. This method of testing drastically reduced the cost of testing compared to testing on actual running engine ducts. Measurements were taken by first recording the results from an untreated duct and then performing the same test with the treatment in place. More testing could be completed using microphone arrays and different configurations [16].

An article from the magazine *Physics World* discusses the novel idea of using phononic crystal lattice structures to manipulate sound (to attenuate sound waves for the purposes of this study). The idea behind using phononic crystal structures is to create a pathway for sound to enter where each wave that travels farther then transfers energy to an interfering wave to the point where the wave can no longer propagate through the material.

Depending on the geometry of the crystal structure, a "band gap" can be created in which a certain band of frequencies cannot propagate within the material making it an effective means of mitigating sound. This method of sound control unfortunately requires larger structures, meters in length, in order to be able to be effective with the human hearing band (20 Hz - 20 kHz). However, the article discusses use with higher frequency waves, i.e. ultrasound, that have shorter wavelengths and therefore would require smaller structures [17].

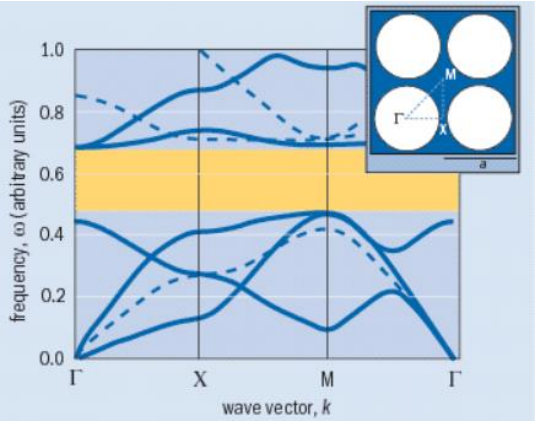

Figure 6: Visual Representation of Band Gaps from Phononic Crystals
Image adapted from a *Physics World* article [17]

A journal study introduces a method for absorbing low and broadband frequencies by taking elements of a traditional Helmholtz resonator and replacing the rigid walls with a light-weight compliant material. The design explored in this article features a cubical structure with a circular opening. Testing was done by using an impedance tube to obtain absorption coefficients. The results of the experiment showed that the presented design had significant effect in absorbing multiple low frequencies. The study states that the multiple compliant walls of the cavity make it an effective broadband absorber. This study concluded that due to its effectiveness and its

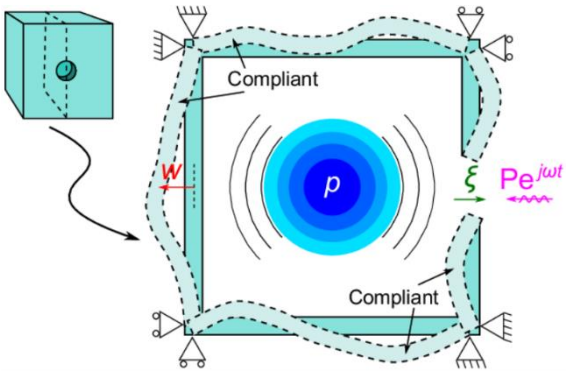

Figure 7: Soft Helmholtz Resonator Absorber Diagram
Image adapted from a study by Cui and Harne [18]

simplistic design, the compliant-material resonator shows great promise in future absorbing sound [18].

A study from 2010 addresses the issues that viscoelastic and poroelastic materials have when attempting to absorb low frequency noise and proposes two simple add-ons as remedies. The study provides a brief outline of the development of the first remedy, Distributed Vibration Absorbers (DVAs), which were derived from a single point mass spring absorber and later evolved into a continuous mass and continuous spring design. The second method labeled heterogenous (HG) blanket utilized a poroelastic material, like a foam, that has multiple masses embedded within and is connected to a base layer. The study claims that the embedded masses are pivotal in aiding the structure dealing with lower frequencies. In the study, both methods exhibit capability of attenuating low frequency noise. Study concluded that the presented methods have substantial evidence in improving future designs that utilize viscoelastic and poroelastic materials [19].

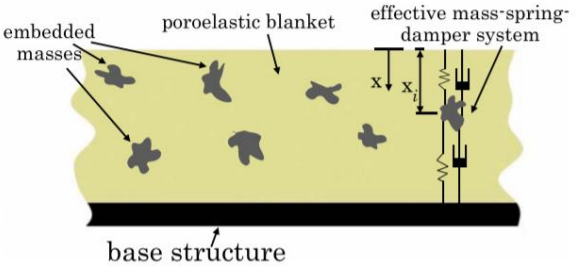

Figure 8: Poroelastic Absorber with Embedded Masses
Image adapted from a study by Fuller and Harne [19]

Chapter 3 – Properties of Materials and Absorption

3.1 Material Density

There are several factors that play a part in determining a material's ability to absorb sound. A material's density plays a large part in a material's absorption coefficient. There have been multiple studies that reveal a negative correlation showing that as a material's

density increases, the material's ability to absorb sound decreases. In a study found in the *Open Journal of Acoustics*, the researchers demonstrate the effects of density on a material's SAC by trialing various densities of fibre board and comparing the results. The results of the study, demonstrating the negative correlation between density and absorption are summarized in the graph shown in **Figure 9** [20]**.**

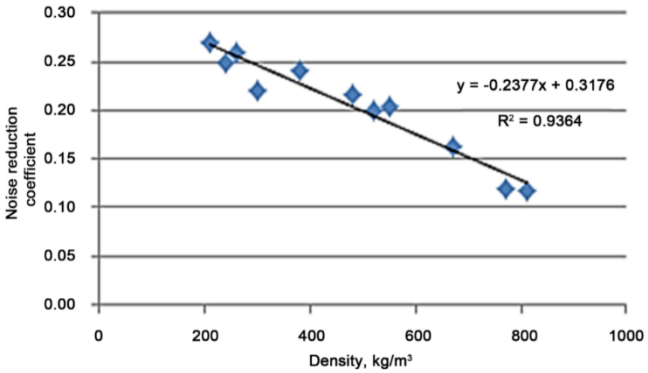

Figure 9: Relationship Between Material Density and Sound Absorption
Image adapted from an *Open Journal of Acoustic's* Study [20]

3.2 Material Porosity

Another factor that affects the ability of a material to absorb sound is how porous a material is. Typically the more porous a material is, the more surface area comes into contact with the soundwave and then more of the energy from the incident wave is converted into heat, thus causing better absorption [21]. A study by Lu et al. sought to explore the effects that pore sizes and amount of porosity has on a material's sound absorption coefficient. This study concluded that pore sizes within the range of 250-1500 μm did not have a significant effect on the sound absorption coefficient. However, they did conclude that the porosity level did affect the frequency range in which the absorption peak

appeared. The results of the experiment can be summarized in **Figure 10** [22].

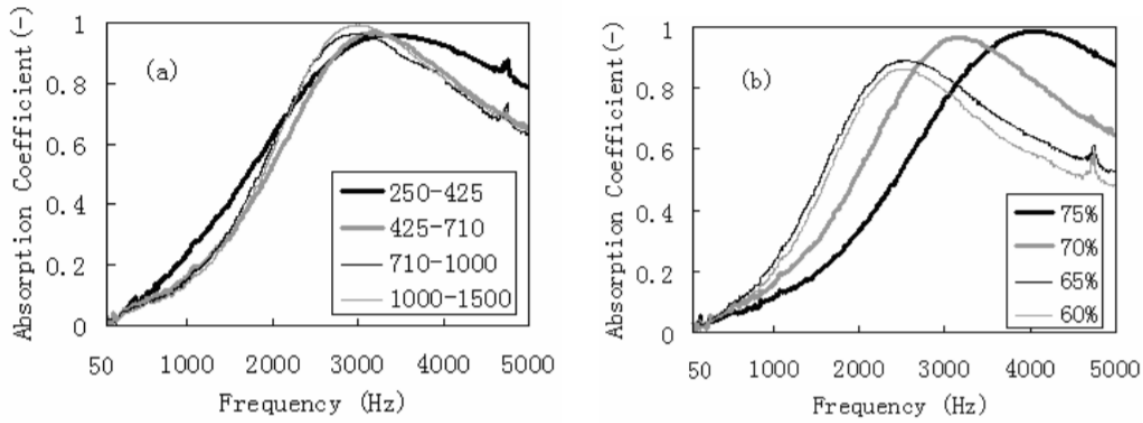

Figure 10: Effects of pore size and porosity on the sound absorption coefficient of porous steel samples with (a) different pore sizes (μm) and a fixed nominal porosity of 70%, and (b) different porosities and a fixed pore size range of 425-710 μm.

Image adapted from study by Lu et al. [22]

3.3 Material Thickness

Material thickness can also play a large part in determining the absorptive capabilities of a material. The thickness of a material has a larger effect on lower frequency absorption. The wavelength of a sound wave gets larger the lower the frequency of the wave. Therefore as the material thickness increases, it has a larger effect on lower frequencies compared to thinner materials. **Figure 11** summarizes an experiment conducted that depicts the absorption coefficient as the used material thickness increases. [21]

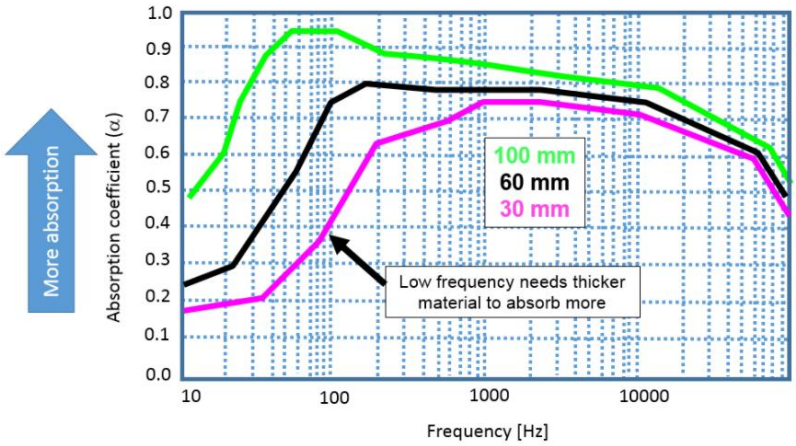

Figure 11: Absorption Performance vs. Material Thickness
Image adapted from siemens.com [21]

Chapter 4 - 3D Printed Sound Panel Fabrication

4.1 CAD Process

In this project, four designs for the sound panels were created using computer-aided design (CAD) software from Autodesk Fusion 360 in order to prep designs for 3D printing. 3D printing is essential for fabricating precise features such as hole size and spacing or bar spacing. The first of these designs features a parabolic dish design, the second uses ideas from phononic crystals, and the third and fourth were unique ideas involving using arrow-like geometry - all of which will be elaborated on in this chapter. Each of these panels was 3D printed using draft resin, courtesy of the Youngstown State University Formlabs 3D printers. Most resin materials have a density around 1.2g/cm3 with the base of the panels typically being at about ½ in thickness.

4.2 Parabolic Disc Panel

The parabolic disc panel was created taking the idea of redirecting sound away as well as absorbing at the same time. The physics of a parabola takes incoming sound waves

and redirect them to point called the focus[23] which can be calculated by the following equation which was adapted from Khan Academy:

$$y = \frac{1}{2(b-k)} * (x-a)^2 + \frac{1}{2}(b+k)$$

Where (a,b) represents the coordinates of the focus and k represents the directrix of the parabola The focus of a parabola is the point in which incoming waves are directed as seen in the image below:

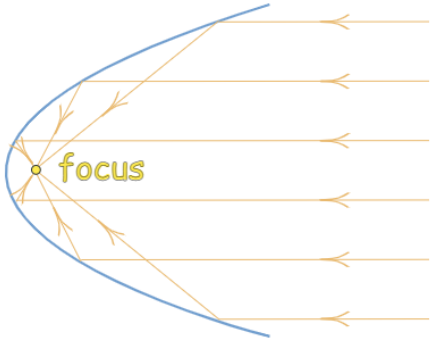

Figure 12: Illustration of Reflected Wave Action,
Image adapted from mathisfun.com

The focus can be adjusted by tweaking the parabola equation above. By rotating the parabola around the vertical axis of the parabola vertex, sound waves can be focused in three dimensions. This is similar to the way that TV satellite dishes as well as parabolic listening devices manipulate incoming waves. Utilizing this property, this design attempts to redirect incoming sound waves to a specific point that is better suited for absorption e.g. the sky (if outdoors), a waveguide, or even the ground. In addition to the focusing properties of the parabolic panel, the panel also features small microperforations which are made possible via 3D printing capabilities[24] which will allow for passage of sound through the panel to help alleviate reverberations throughout the material produced mainly

from lower frequencies. Images of the parabolic disc panel can be seen in **Figure 13** and **Figure 14** shows the printed model.

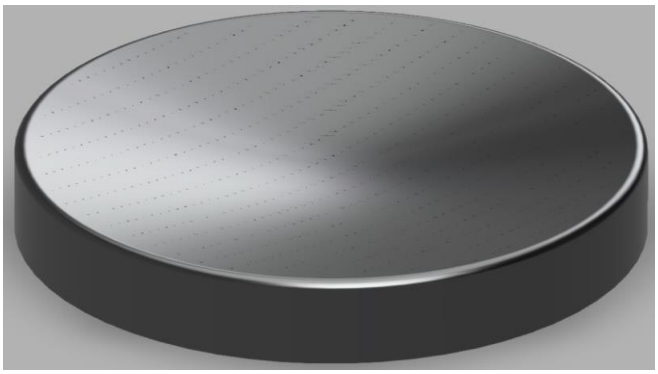

Figure 13 CAD Drawing of Parabolic Disc Panel

Figure 14: Draft Resin 3D printed Parabolic Disc Panel

4.3 Derivative Phononic Crystal Panel

Phononic crystals (PCs) are usually defined as artificial structures made of periodic arrangement of scatterers embedded in a matrix[25]. The idea behind using a phononic crystal for sound absorption is that as sound waves are emitted into the array of "scatterers", in this case pillars. The sound waves will be reflected into each other as they progress through the structure causing destructive interference and therefore dissipating the waves. The panel designed in this experiment utilizes a 2 dimensional crystalline configuration similar to the illustration in **Figure 15**:

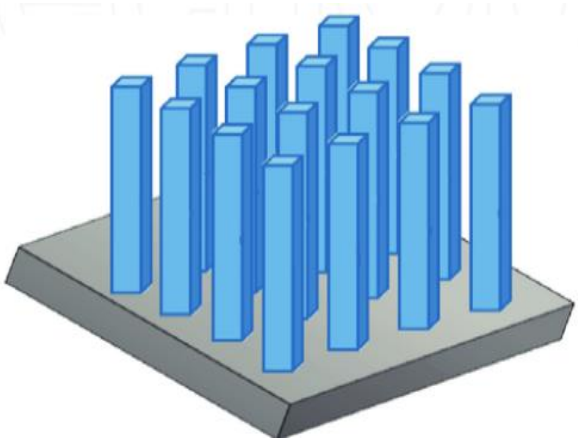

Figure 15: 2D Crystalline Phononic Structure
Image adapted from researchgate.net

Instead of a vertical array of rectangular pillars, this panel features an array of cylindrical pillars within a square casing. A CAD drawing of the second panel derived from the phononic crystal concept can be seen in **Figure 16** and **Figure 17** shows the printed model.

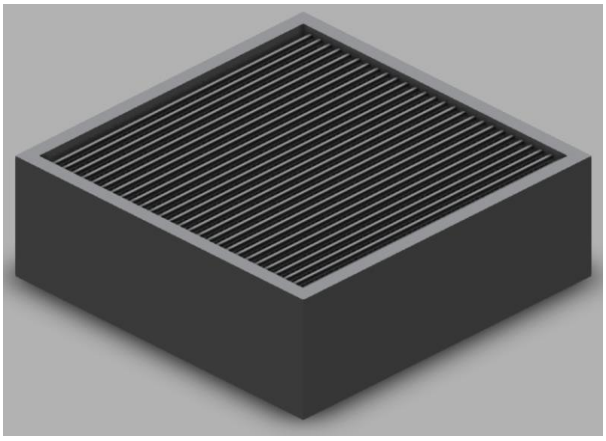

Figure 16: CAD Drawing of 2D Phononic Crystal Panel

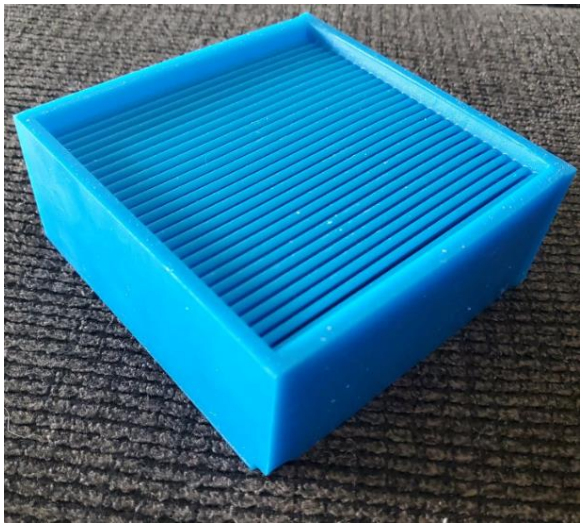

Figure 17: Draft Resin 3D printed Phononic Crystal Panel

4.4 Conical Arrow Panel

The design of the conical arrow panel was developed with the idea of allowing sound to easily pass into the panel and to then trap the sound underneath the conical tops of the "arrows". This panel features an array of cylindrical bases with a conical head, similar to an umbrella, giving the appearance of arrows pointing upward from a side view. The tip of the conical arrows on the panel all have holes that lead down into a tapered hole to add additional spaces to trap sound inside the conical arrow structures. **Figure 18-A** shows the CAD drawing of the conical arrow panel and **Figure 18-B** and **Figure 18-C** show different views of the individual conical structures appear on the panel. **Figure 19** shows the actual printed model of the conical arrow panel.

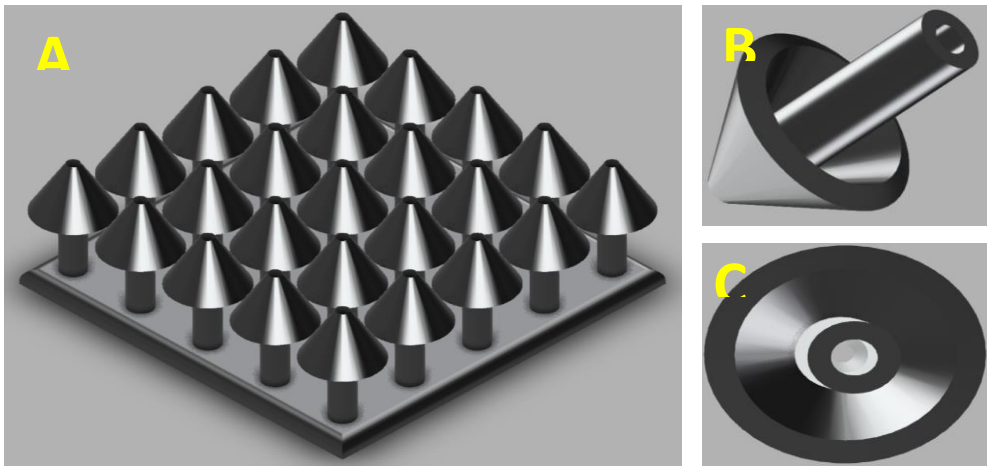

Figure 18-A: CAD Drawing of Conical Arrow Panel
Figure 18-B: CAD Isometric Drawing of Underside of Single Conical Structure
Figure 18-C: CAD Drawing of Underside of Single Conical Structure

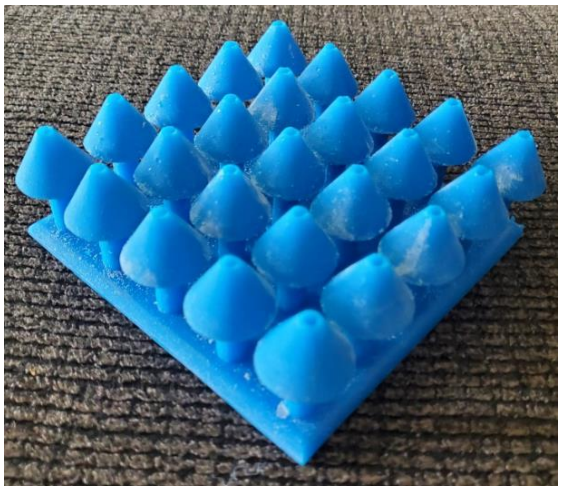

Figure 19: Draft Resin 3D printed Conical Arrow Panel

4.5 Block Arrow Panel

The block arrow panel design was an adaptation of the conical arrow panel and therefore has the same method intended for controlling sound. The feature that sets the block arrow panel apart from the conical arrows is the shape of the "arrow" structures assorted in a matrix. These arrow-like structures were designed to have flat surfaces and from a top view have an uneven surface to ideally promote the diffusion of sound waves. The waves that pass through the cracks will theoretically be trapped under the arms of the

arrow structures. **Figure 20-A** shows the CAD drawing of the block arrow panel and **Figure 20-B** and **Figure 20-C** show different views of the individual arrow-like structures appear on the panel. **Figure 21** shows the actual printed model of the block arrow panel.

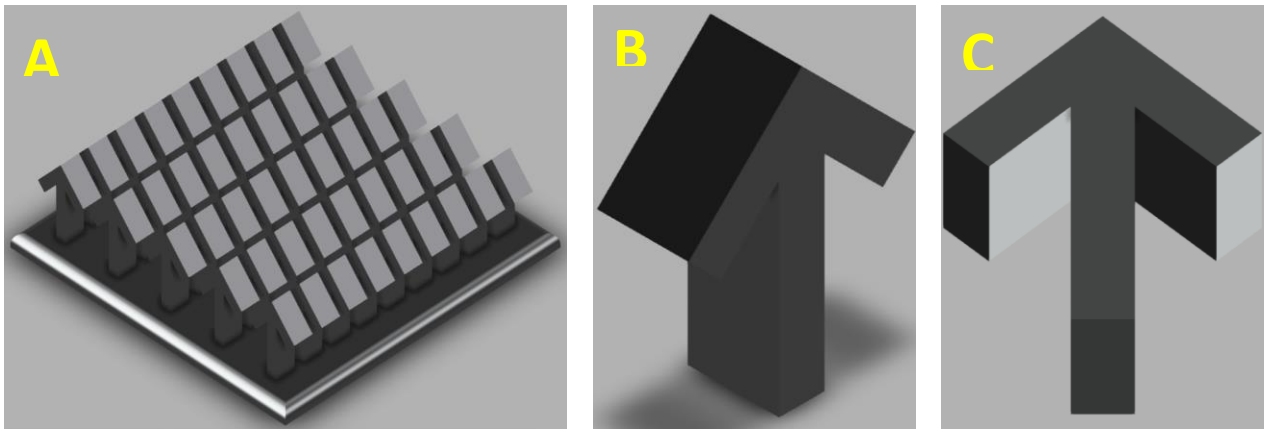

Figure 20-A: CAD Drawing of Block Arrow Panel
Figure 20-B: CAD Drawing of Single Block Arrow Structure
Figure 20-C: CAD Drawing of Underside of Single Block Arrow Structure

Figure 21: Draft Resin 3D printed Block Arrow Panel

Chapter 5 - Experimental Set-Up

5.1 Acoustic Testing Background

Testing acoustic paneling is a straightforward process. Typically, professional acoustic testing is carried out in reverberation chambers. A reverberation chamber is a chamber that is designed to encourage reverberations or echoes by limiting the number of parallel surfaces as well as limiting absorptive materials. The idea behind using a reverberation chamber is to measure how long the reverberation lasts after a sound is played. This measurement compared to a control will give a good indication of how effective an acoustic treatment is in absorbing noise. The longer the reverberation lasts after the sound has stopped, the less absorptive the material is considered to be. Further testing could be done in order to determine if there are specific frequencies that are more affected by specific acoustic treatment. A good way to determine this is to subject the acoustic treatment to pink noise. Pink noise is a signal where each octave carries equal sound energy and is therefore great for analyzing frequencies within the human hearing spectrum (20 Hz to 20,000 Hz) [26].

5.2 Experimental Software and Materials

Audacity® was the software used to perform all of the audio processes including: playing sound files, recording sound wave data, and performing acoustical analyses. Audacity is a free digital audio workstation (DAW) that also contains a vast repertoire of analytical processes including plotting frequency spectra used in this project. A LE BOSE™ Soundlink Micro speaker was used to emit audio signals and a FIFINE® K669B USB microphone was used to record audio. Two plastic Sterilite® bins were used to create

an enclosure for testing. A rubber gasket was used to hold the microphone in place while creating a seal and duct tape was used to fasten everything together.

5.3 Creating a Reverberation Chamber

The design of this experiment was modeled off of a study by Rey et al. where a small sized reverberation chamber was used to measure the absorption of a sound panel [27]. A miniature reverberation chamber was made out of two $36\frac{5}{8}$" L x 21" W x $19\frac{1}{2}$" H plastic Sterilite® bins. One side (lengthwise) from each of the bins was cut off using a box cutter and then the open ended sides were put together and fastened with duct tape in order to double the volume of the bin. This was done create more space to allow sound waves to travel. Next, a hole was cut in the base of the combined bin structure to allow for the microphone to be inserted into the enclosure. The hole was slightly bigger than the diameter of the microphone (1.75 in) so that a rubber gasket could be inserted to create an airtight seal as well as provide a slight buffer for the microphone from picking up vibrations through the material of the plastic bin itself. The next step was to fasten the speaker to the opposite end of the base of the combined plastic bin. This was done by simply taping the speaker to the base and ensuring not to obstruct the opening to avoid any sort of distortion of sound. A graphical depiction of the testing apparatus can be seen in **Figure 22** and **Figure 23**. With the testing apparatus completed, then started the data collection process.

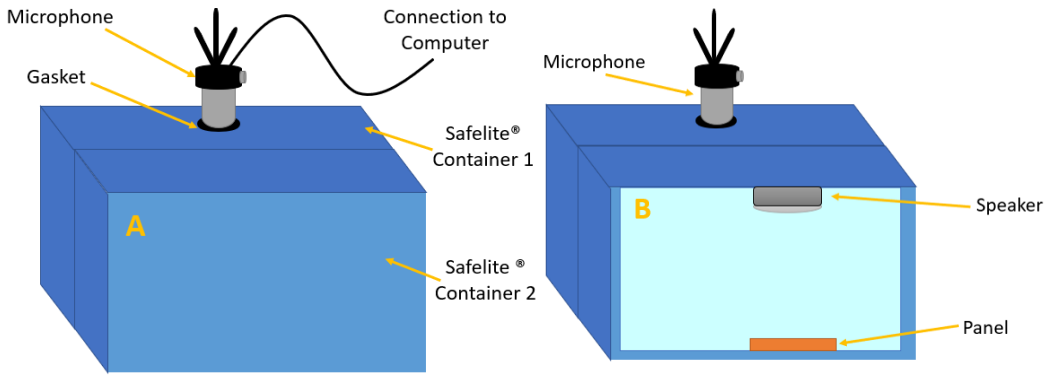

Figure 22-A: Outside View of Testing Apparatus
Figure 22-B: Underside View of Inside of Testing Apparatus

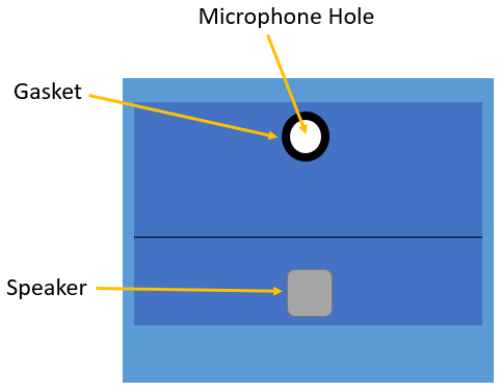

Figure 23: Underside View of Inside of Testing Apparatus

5.4 Data Collection Process

In order to gather data, two sound files were selected to do each of the trials. The first sound file is labeled *Point Source POP*. This file contains the sound of someone popping a balloon with a needle. This specific sound was chosen because it is very useful for determining the amount of time it takes for the reverberations to decay by a level 60 dB also known as the RT-60 which is, for the purpose of this report, inaudible to the human ear. This means that the lower the RT-60, the less the environment is suited for reverberations and is better at absorbing sound. The other sound file that was used was a 10 second clip of pink noise. This, as stated before, is useful when looking at a frequency

spectrum to determine how each frequency is affected when exposed to an environment. This is useful to look at because it is possible that certain environments may have a resonant frequency in which a certain frequency is boosted, or it is possible that only certain frequencies are affected in comparison to others.

The casing that was described in **Section 5.3** was placed with the opening against tile flooring to enclose an area for testing. First, the control data, which consisted of the empty casing (no panels) was done. To do this, the *Point Source POP* sound file was played from the speaker that was attached via the Audacity software. As the popping sound played, it was recorded using the microphone to determine how the environment of the casing affected the sound waves. This was repeated so that there were a total of five control recordings to be subjected for analysis. After collecting all of the *Point Source POP* data, the process was repeated another five times, but instead playing the 10 seconds of pink noise through the speaker and recording it with the microphone which resulted in another five pink noise control data points.

After collecting all of the data for the controlled setting, the casing was lifted to place the first panel, the parabolic disc panel, underneath the speaker and then the casing was placed against the ground again. The same *Point Source POP* file was played and recorded five separate times as well as five recordings of the pink noise file to be used for analysis. This procedure was repeated for each of the remaining panels in the respective order: Phononic Crystal Panel, Conical Arrow Panel, and Block Arrow Panel. After all the data was recorded, it was time to analyze.

5.5 Data Analysis and Results

The density of a material plays a large part in its effectiveness in absorbing sound [20]. To eliminate this factor, all panels were all made from the same draft resin material, with the same density. Therefore, the purpose of this analysis is to understand the effect of panel shape on the absorption of sound. The experiment was conducted using the sound of a balloon being popped by a needle, labeled as Point Source POP. One way to measure the effectiveness of an absorptive material is to measure the reverberation time (RT) of the encasement with the respective panel. RT was thus used as an objective approximation of the sound-limiting capabilities of the 3D printed sound panels. Specifically, in this study, the amount of time it took for the reverberation to decrease by 60 dB (essentially no noise to the human ear), also known as the RT-60, was approximately measured from the sound wave files. Five separate RT-60 data points were collected from each of the four panel shapes as well as for a control (See **Table 1**). The experiment was then repeated using a Pink Noise sound burst (See **Table 2**).

A one-way analysis of variance (ANOVA) was used to determine whether the Point Source POP null hypothesis is true. (See **Table 3**). The Point Source POP null hypothesis is as follows:

$$\mu_c = \mu_{pd} = \mu_{pc} = \mu_{ca} = \mu_{ba}$$

where μ is the population mean, c is the control group, pd is the parabolic disc group, ca is conical arrow group and ba is block arrows. The p-value =0.0000122 of the ANOVA output tells us whether to accept or reject the above null hypothesis. A 95% confidence level was used. Therefore, the relevant p-value is 0.05. Since the Point Source POP value

is lower than 0.05, the null hypothesis is rejected, meaning that there is at least one inequality between the groups. Additionally, the critical value of the Point Source POP ANOVA table is examined. The F value (14.177) is greater than the critical value (2.866). (See **Table 3**). Therefore, this again indicates the necessity to reject the null hypothesis, validating again that at least one group is statistically significant and not equal.

The data was further analyzed by comparing each design group separately against the control group using a t-test. The two-sample t-test was run four times to compare the mean of the control group to one of the four panel design groups (parabolic disc, phononic crystal, conical arrows or block arrows) to determine if there is a significant difference (See **Appendix A** for t-test tables of each comparison). Using the same Point Source POP null hypothesis as stated above ($\mu_c = \mu_{pd} = \mu_{pc} = \mu_{ca} = \mu_{ba}$), the p-value is examined to determine whether to accept or reject.

Table 1: Summary Table of Point Source POP RT-60 t-tests

Group 1	Group 2	p-value	t- value	t-Critical	Bonferoni #	Determination
Control	Parabolic Disc	0.00097	5.06488	2.30600	0.025	Reject H_0
Control	Phononic Crystal	0.00414	3.96594	2.30600	0.025	Reject H_0
Control	Conical Arrows	0.00202	4.49337	2.30600	0.025	Reject H_0
Control	Block Arrows	0.00973	3.37403	2.30600	0.025	Reject H_0

For each Point Source POP t-test, the p-value is greater than 0.05, indicating to reject the null hypothesis, stating that the means of the two groups are the same. In addition, the t-values are greater than the critical value, again indicating to reject the null hypothesis. The Bonferroni correction number was then applied to help adjust for error. In each instance the p-value was less than the Bonferroni correction number, indicating that there is a statistical significance and the rejection of the null hypothesis is valid. Rejection of the null

hypothesis indicates that the RT-60 time of the design shape panel is significantly different than the control. Looking at the mean RT-60 mean values for each panel design, the parabolic disc has the lowest mean.

Table 2: Summary Table of Point Source POP values.

Point Source POP Group	Mean	Standard Deviation
Parabolic Disc	0.5208	0.0047
Conical Arrows	0.5230	0.0085
Phononic Crystal	0.5304	0.0037
Block Arrows	0.5328	0.0088
Control	0.5632	0.0181

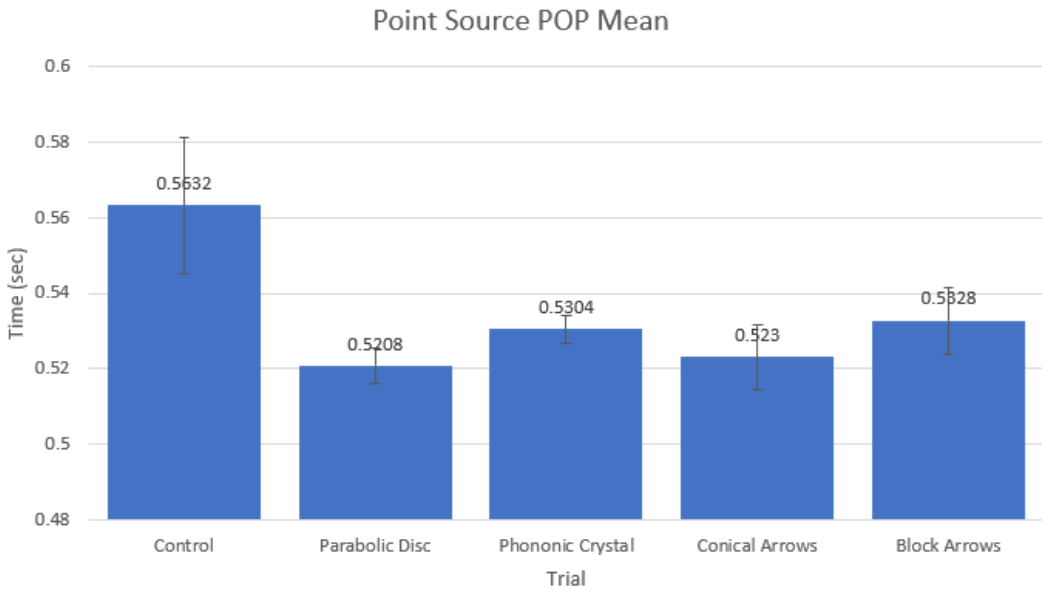

Figure 24: Point Source POP Mean Summary with Error Bar

All of the shape design panels have an RT-60 mean less than that of the control which suggests that the resin panel, regardless of shape, allows for more sound absorption than without a panel. The parabolic disc design allowed for the most sound absorption as seen from the lowest RT-60 mean value. The standard deviation of the parabolic disc sample data is low meaning the data is closely related to the mean and is therefore more reliable.

The ANOVA table analysis with a 95% confidence level was also used for the Pink Noise data groups to ultimately not reject the null hypothesis. (See **Table A.8** in **Appendix A**). As seen with the Point Source POP, null hypothesis for Pink Noise is as follows:

$$\mu_c = \mu_{pd} = \mu_{pc} = \mu_{ca} = \mu_{ba}$$

where μ is the population mean, *c* is the control group, *pd* is the parabolic disc group, *ca* is conical arrow group and *ba* is block arrows. The Pink Noise ANOVA table produced a p-value of 0.0508 output tells us whether to accept or reject the above null hypothesis. Under this data set, the p-value is slightly higher than 0.05, meaning that the null hypothesis cannot be rejected. To further support this, the 2.853 F value is slightly lower than the critical value of 2.866. (See **Table 4**).

To further validate the finding to not reject the null hypothesis, a two-tailed t-test was run on the Pink Noise control versus each of the design panels (See **Appendix A** for full t-test tables of each comparison). Using the same Pink Noise null hypothesis as stated above ($\mu_c = \mu_{pd} = \mu_{pc} = \mu_{ca} = \mu_{ba}$), the p-value, t-critical value were examined to see if these values also supported to not reject the null hypothesis.

Table 3: Summary Table of Pink Noise t-tests. Taken from t-test in **Appendix A**

Group 1	Group 2	p-value	t- value	t-Critical	Bonferoni #	Determination
Control	Parabolic Disc	0.0717	2.0750	2.30600	0.025	Do Not Reject H_0
Control	Phononic Crystal	0.0476	2.3371	2.30600	0.025	Do Not Reject H_0
Control	Conical Arrows	0.1303	1.6856	2.30600	0.025	Do Not Reject H_0
Control	Block Arrows	0.0625	2.1626	2.30600	0.025	Do Not Reject H_0

For the Parabolic Disc, Conical Arrow and Block Arrow, the p-values were greater than .05 and the t-value was less than the critical value. Again supporting to not reject the null

hypothesis. The Phononic Crystal had a p-value less than 0.05 and had a t-value slightly higher than the critical value. However, when correcting for error with the Bonferroni number, this too showed not to reject the null hypothesis. Not rejecting the null hypothesis of the Pink Noise test indicates that there is not a significant difference between the mean of the control vs the mean of each of the design panel. Therefore, the absorptive properties of the four panel designs do not appear to be much better than that of the control with no sound panel.

In addition to recording data for the RT-60 of each panel, a frequency spectrum analysis was generated using the Audacity® software (see **Appendix B** for spectra). This was done using a *Pink Noise* sound file that was generated via software. Five separate recordings were taken for each panel, similar to the data collection process with the *Point Source POP* recordings but instead using pink noise. A total of five trials were done for each panel resulting in a total of 20 different spectra. Based on visual inspection of the frequency spectra, each panel had very similar results. Of note, in comparison to the Control, the Phononic Crystal, Conical Arrow, and Block Arrow panels had a maximum amplitude of -28 dB whereas the Control had a maximum amplitude of -23 dB. This shows that these panels were effective in reducing the overall sound pressure level that the microphone experienced by 5 dB. Unlike the other panels, the Parabolic Disc panel appeared to have had the opposite effect resulting in a maximum amplitude of -22 dB which is even higher than the Control. This could be the result of the geometry of the paraboloid structure of the panel focusing the reflected waves into the mic, therefore creating a greater sound pressure level at the actuator of the microphone. A summary of these results can be

seen int **Table 4** and the frequency spectra graphs from which the data came from can be seen in **Appendix B**.

Table 4: Summary of Pink Noise Frequency Spectra Peaks at ~100 Hz

Pink Noise Highest Peak at ~100Hz (Units in dB)						
Panel	Trial 1	Trial 2	Trial 3	Trial 4	Trial 5	Average
Control	-23	-22	-23	-22	-23	-22.6
Parabolic Disc	-22	-23	-23	-23	-23	-22.8
Phononic Crystal	-28	-28	-28	-28	-28	-28
Conical Arrow	-28	-28	-28	-28	-28	-28
Block Arrow	-28	-28	-28	-28	-28	-28

Chapter 6 - Conclusions and Future Work

6.1 Conclusion

Noise pollution is a growing concern due to the increasing rate of urbanization. There are some methods in existence that are sufficient in reducing noise pollution. However, they are expensive, and due to the continuous rise in the noise floor, they will not be able to remedy the solution in the future. This study focused on exploring some possible augmentations, adaptations, and/or replacements to current sound absorbers by exploring the effectiveness of four different designs of 3-D printed acoustic paneling in absorbing sound. A cheap imitation of a reverberation chamber was created out of plastic bins used to test the 3D-printed acoustic panels in question. All four panels have statistical significance in decreasing reverberation time. The use of these designs as an absorptive panel can be extrapolated to reducing reverberations along the highway or in a private residence. Additionally, after analyzing frequency spectra from the Pink Noise trials, the phononic crystal, conical arrow and block arrow panels reduced the sound pressure level

within the encasement showing some aptitude in being a sound absorber. This study provides further documentation that 3D-printed acoustic paneling in various structural configurations can be a cost effective and efficient method to absorb noise of audible frequencies as well as reduce sound intensity. The data presented have potential for implications in the public health sector, in commercial use and residential use.

6.2 Application Economics

This section focuses on the economics of using these panels in actual applications. By using the services of sd3d.com**,** a quote for a 6" by 6" panel of each type was given and then the price for each panel was extrapolated to cover the walls of a 10' by 10' by 10' room as well as a 14 ft (average height of highway sound barriers in Ohio [28]), mile long highway barrier. The parabolic disc panel, based on the price extrapolation, would be the most cost effective option of the panels assuming a cost of $0.15/g of polylactic acid (PLA) material. The average cost of a highway sound barrier in Ohio is $1.8 million dollars. A mile long highway sound barrier made of PLA parabolic panels was estimated to cost approximately $5 million, however this does not take into consideration price reductions due to mass production of panels.

Table 5: Summary of Application Economics

	Parabolic Disc	Phononic Crystal	Conical Arrow	Block Arrow
Weight 6" panel (g)	113	261	159	136
Base Cost for 6" panel (assuming $0.15/g)	$ 16.95	$ 39.15	$ 23.85	$ 20.40
14' long barrier (assuming $0.15/g)	$ 5,011,776.00	$ 77,172,480	$ 7,051,968.00	$ 6,031,872.00
10'x10'x10' room (assuming $0.15/g)	$ 27,120.00	$ 62,640.00	$ 38,160.00	$ 32,640.00

6.3 Future Work

Future work could be done by examining how some of the panels interact with each other. For example, if using the parabolic disc panel to focus incoming noise to another panel such as the phononic crystal panel. Another area of interest would be the use of soft 3D printing materials. One example that was mentioned in **Chapter 2** was a take on a Helmholtz resonator that was made out of a soft material that had exceptional results in absorbing sound. Finally, future work could be done to determine if the angle or positioning of the sound panel within the encasement affected the overall sound reduction.

In doing this study, there were several limiting factors that could have impacted the results of the data. The first is the size of the 3D printed panels. Due to the limitations of the 3D printers available, the panels had to remain quite small. Having larger panels could play a role in how well the panel absorbed sound. Another aspect of the study that could have had an effect on the results is the reverberation chamber fashioned out of plastic bins. Having an actual echo chamber with a low ambient noise floor would produce an environment that would produce more accurate results from the panels; however, access to an echo chamber was unavailable. In addition to the lack of larger panels and a reverberation chamber panels the absorption coefficients could not be determined due to the cost of an impedance tube and lack thereof.

References

[1] H. Jariwala, H. J. Jariwala, H. S. Syed, M. J. Pandya, and Y. M. Gajera, "Noise Pollution & Human Health: A Review," 2017. Accessed: Mar. 31, 2021. [Online]. Available: https://www.researchgate.net/publication/319329633.

[2] T. Münzel, T. Gori, W. Babisch, and M. Basner, "Cardiovascular effects of environmental noise exposure," *European Heart Journal*, vol. 35, no. 13. Oxford University Press, p. 829, 2014, doi: 10.1093/eurheartj/ehu030.

[3] "Noise & Health - Noise Free America: A Coalition to Promote Quiet." https://noisefree.org/noise-health/ (accessed Apr. 01, 2021).

[4] A. Mital and A. S. Ramakrishnan, "Effectiveness of noise barriers on an interstate highway: a subjective and objective evaluation.," *J. Hum. Ergol. (Tokyo).*, vol. 26, no. 1, pp. 31–38, Jun. 1997, doi: 10.11183/jhe1972.26.31.

[5] W. J. Harris, J.; J. Lynn Helms;, R. A. Peck, J.; Arthur E, and J. R. Teele, "HIGHWAY NOISE BARRIERS," Allen & Hamilton, Inc, 1980.

[6] Meryl Davids Landau, "On Highway Noise Barriers, the Science Is Mixed. Are There Alternatives?," Dec. 27, 2017. https://undark.org/2017/12/27/highway-noise-barrier-science/ (accessed Apr. 01, 2021).

[7] "Average Unit Cost By Year - Trends - Inventory - Noise Barriers - Noise - Environment - FHWA." https://www.fhwa.dot.gov/Environment/noise/noise_barriers/inventory/trends/ttable2.cfm (accessed Apr. 01, 2021).

[8] J. Mei, G. Ma, M. Yang, Z. Yang, W. Wen, and P. Sheng, "Dark acoustic metamaterials as super absorbers for low-frequency sound," *Nat. Commun.*, vol. 3,

no. 1, pp. 1–7, Mar. 2012, doi: 10.1038/ncomms1758.

[9] Z. Liu, J. Zhan, M. Fard, and J. L. Davy, "Acoustic measurement of a 3D printed micro-perforated panel combined with a porous material," *Meas. J. Int. Meas. Confed.*, vol. 104, pp. 233–236, Jul. 2017, doi: 10.1016/j.measurement.2017.03.032.

[10] M. R. A. Muhammad Fakrul Syahid Che Hamid, A. Putra, G.H. Kassim, "3D-printed lattice structure as sound absorber," *Proceedings of Mechanical Engineering Research Day 2019*, 2019. https://books.google.com/books?hl=en&lr=&id=DkqnDwAAQBAJ&oi=fnd&pg=PA287&dq=3d-printed+lattice+structure+as+sound+absorber+muhammad+fakrul&ots=2LsnRur1t9&sig=ceTnbrbvStA2s-lhQKC5Xl6etEc#v=onepage&q=3d-printed lattice structure as sound absorber muhammad f (accessed Apr. 01, 2021).

[11] M. A. A. Farah Liana, "Experimental determination of sound absorption coefficient of green materials polymer from different compositions," *Proceedings of Mechanical Engineering Research Day 2019*, 2019. https://books.google.com/books?hl=en&lr=&id=DkqnDwAAQBAJ&oi=fnd&pg=PA289&dq=experimental+determination+of+sound+absorption+coefficient+of+green+materials+polymer+from+different+compositions&ots=2LsnRus4m6&sig=2rCqLQoRHODotRPjBPGZITXdfKg#v=onepage&q&f=fals (accessed Apr. 01, 2021).

[12] A. Arjunan, "Targeted sound attenuation capacity of 3D printed noise cancelling waveguides," *Appl. Acoust.*, vol. 151, pp. 30–44, Aug. 2019, doi: 10.1016/j.apacoust.2019.03.008.

[13] A. Lavie, A. Leblanc, and A. Ba, “Soft 3D printed membrane type-acoustic metamaterials SOFT 3D PRINTED MEMBRANE TYPE-ACOUSTIC METAMATERIALS,” 2016. Accessed: Mar. 31, 2021. [Online]. Available: https://www.researchgate.net/publication/306917346.

[14] P. Cobo, C. de la Colina, E. Roibás-Millán, M. Chimeno, and F. Simón, “A wideband triple-layer microperforated panel sound absorber,” *Compos. Struct.*, vol. 226, p. 111226, Oct. 2019, doi: 10.1016/j.compstruct.2019.111226.

[15] Yang *et al.*, “3D Printing of Polymeric Multi-Layer Micro-Perforated Panels for Tunable Wideband Sound Absorption,” *Polymers (Basel).*, vol. 12, no. 2, p. 360, Feb. 2020, doi: 10.3390/polym12020360.

[16] “NASA Technical Reports Server (NTRS).” https://ntrs.nasa.gov/citations/19920005565 (accessed Mar. 31, 2021).

[17] T. Gorishnyy, M. Maldovan, C. Ullal, and E. Thomas, “Sound ideas,” *Physics World*, vol. 18, no. 12. Institute of Physics Publishing, pp. 24–29, Dec. 01, 2005, doi: 10.1088/2058-7058/18/12/30.

[18] S. Cui and R. L. Harne, “Soft Materials with Broadband and Near-Total Absorption of Sound,” *Phys. Rev. Appl.*, vol. 12, p. 64059, 2019, doi: 10.1103/PhysRevApplied.12.064059.

[19] C. R. Fuller and R. L. Harne, “Passive distributed vibration absorbers for low frequency noise control,” 2010.

[20] A. Nandanwar, M. C. Kiran, and K. Ch Varadarajulu, “Influence of Density on Sound Absorption Coefficient of Fibre Board,” *Open J. Acoust.*, vol. 7, pp. 1–9, 2017, doi: 10.4236/oja.2017.71001.

[21] “Sound Absorption.” https://community.sw.siemens.com/s/article/sound-absorption (accessed Mar. 31, 2021).

[22] M. Lu, C. Hopkins, Y. Zhao, and G. Seiffert, “Sound Absorption Characteristics of Porous Steel Manufactured by Lost Carbonate Sintering,” 2009.

[23] G. Kaplan, “Parabolic Connections Linking History, Art, Acoustics, and Mathematics.”

[24] D.-Y. Maa, “Potential of microperforated panel absorber,” *J. Acoust. Soc. Am.*, vol. 104, no. 5, pp. 2861–2866, Nov. 1998, doi: 10.1121/1.423870.

[25] A. C. Hladky-Hennion, “Phononic crystal (PC) applications of ATILA,” in *Applications of ATILA FEM Software to Smart Materials: Case Studies in Designing Devices*, Elsevier Ltd., 2012, pp. 190–202.

[26] “Pink Noise | Hyperacusis Focus.” https://hyperacusisfocus.org/pink-noise/#whitevpink (accessed Mar. 31, 2021).

[27] R. Del Rey, J. Alba, L. Bertó, and A. Gregori, “Small-sized reverberation chamber for the measurement of sound absorption,” *Mater. Constr.*, vol. 67, no. 328, p. 139, Oct. 2017, doi: 10.3989/mc.2017.07316.

[28] “Noise Barrier Construction by State by Average Height - Summary - Inventory - Noise Barriers - Noise - Environment - FHWA.” https://www.fhwa.dot.gov/Environment/noise/noise_barriers/inventory/summary/stable713.cfm (accessed Apr. 22, 2021).

Appendix A: Statistical Analyses

Table A.1: Point Source POP RT-60 Trial Results Summary (units in seconds {s})

Point Source POP				
Control	Parabolic Disc	Phononic Crystal	Conical Arrows	Block Arrows
0.559	0.527	0.528	0.522	0.53
0.588	0.524	0.533	0.533	0.52
0.544	0.516	0.535	0.513	0.536
0.55	0.517	0.526	0.53	0.534
0.575	0.52	0.53	0.517	0.544

Table A.2: Point Source POP ANOVA Test Summary

Anova: Single Factor Point Source POP						
SUMMARY						
Groups	Count	Sum	Average	Variance		
Control	5	2.816	0.5632	0.0003287		
Parabolic Disc	5	2.604	0.5208	0.0000217		
Phononic Crystal	5	2.652	0.5304	0.0000133		
Conical Arrows	5	2.615	0.523	7.15E-05		
Block Arrows	5	2.664	0.5328	7.72E-05		
ANOVA						
Source of Variation	SS	df	MS	F	P-value	F crit
Between Groups	0.005811	4	0.0014528	14.17681499	1.21853E-05	2.866081
Within Groups	0.00205	20	0.0001025			
Total	0.007861	24				
H0: ucontrol = uPD = uPhC = uCA = uBA						
Reject Ho						

Table A.3: Point Source POP Two Tail t-Test (Control – Parabolic Disc)

Point Source POP		
t-Test: Two-Sample Assuming Equal Variances		
	Control	Parabolic Disc
Mean	0.5632	0.5208
Variance	0.0003287	0.0000217
Observations	5	5
Pooled Variance	0.0001752	
Hypothesized Mean Difference	0	
df	8	
t Stat	5.064875915	
P(T<=t) one-tail	0.000485579	
t Critical one-tail	1.859548038	
P(T<=t) two-tail	0.000971158	
t Critical two-tail	2.306004135	

Table A.4: Point Source POP Two Tail t-Test (Control – Phononic Crystal)

Point Source POP		
t-Test: Two-Sample Assuming Equal Variances		
	Control	Phononic Crystal
Mean	0.5632	0.5304
Variance	0.0003287	0.0000133
Observations	5	5
Pooled Variance	0.000171	
Hypothesized Mean Difference	0	
df	8	
t Stat	3.965936834	
P(T<=t) one-tail	0.002071217	
t Critical one-tail	1.859548038	
P(T<=t) two-tail	0.004142434	
t Critical two-tail	2.306004135	

Table A.5: Point Source POP Two Tail t-Test (Control – Conical Arrows)

Point Source POP		
t-Test: Two-Sample Assuming Equal Variances		
	Control	Conical Arrows
Mean	0.5632	0.523
Variance	0.0003287	7.15E-05
Observations	5	5
Pooled Variance	0.0002001	
Hypothesized Mean Difference	0	
df	8	
t Stat	4.493373432	
P(T<=t) one-tail	0.001009858	
t Critical one-tail	1.859548038	
P(T<=t) two-tail	0.002019715	
t Critical two-tail	2.306004135	

Table A.6: Point Source POP Two Tail t-Test (Control – Block Arrows)

Point Source POP		
t-Test: Two-Sample Assuming Equal Variances		
	Control	Block Arrows
Mean	0.5632	0.5328
Variance	0.0003287	7.72E-05
Observations	5	5
Pooled Variance	0.00020295	
Hypothesized Mean Difference	0	
df	8	
t Stat	3.374030935	
P(T<=t) one-tail	0.004863647	
t Critical one-tail	1.859548038	
P(T<=t) two-tail	0.009727295	
t Critical two-tail	2.306004135	

Table A.7: Pink Noise RT-60 Trial Results Summary (units in seconds {s})

Pink Noise				
Control	Parabolic Disc	Phononic Crystal	Conical Arrows	Block Arrows
0.18	0.179	0.159	0.188	0.122
0.181	0.152	0.134	0.146	0.159
0.17	0.147	0.148	0.152	0.153
0.166	0.159	0.15	0.161	0.174
0.245	0.14	0.169	0.159	0.153

Table A.8: Pink Noise ANOVA Test Summary

Anova: Single Factor Pink Noise						
SUMMARY						
Groups	Count	Sum	Average	Variance		
Control	5	50.942	10.1884	0.0010423		
Parabolic Disc	5	50.777	10.1554	0.0002223		
Phononic Crystal	5	50.76	10.152	0.0001705		
Conical Arrows	5	50.806	10.1612	0.0002597		
Block Arrows	5	50.761	10.1522	0.0003587		
ANOVA						
Source of Variation	SS	df	MS	F	P-value	F crit
Between Groups	0.004685	4	0.0011713	2.852057463	0.050775781	2.866081
Within Groups	0.008214	20	0.0004107			
Total	0.012899	24				
H0: ucontrol = uPD = uPhC = uCA = uBA						
Reject Ho						

Table A.9: Pink Noise Two Tail t-Test (Control – Parabolic Disc)

Pink Noise		
t-Test: Two-Sample Assuming Equal Variances		
	Control	Parabolic Disc
Mean	0.1884	0.1554
Variance	0.0010423	0.0002223
Observations	5	5
Pooled Variance	0.0006323	
Hypothesized Mean Difference	0	
df	8	
t Stat	2.075020317	
P(T<=t) one-tail	0.035833878	
t Critical one-tail	1.859548038	
P(T<=t) two-tail	0.071667755	
t Critical two-tail	2.306004135	

Table A.10: Pink Noise Two Tail t-Test (Control – Phononic Crystal)

Pink Noise		
t-Test: Two-Sample Assuming Equal Variances		
	Control	Phononic Crystal
Mean	0.1884	0.152
Variance	0.0010423	0.0001705
Observations	5	5
Pooled Variance	0.0006064	
Hypothesized Mean Difference	0	
df	8	
t Stat	2.337178011	
P(T<=t) one-tail	0.023812515	
t Critical one-tail	1.859548038	
P(T<=t) two-tail	0.04762503	
t Critical two-tail	2.306004135	

Table A.11: Pink Noise Two Tail t-Test (Control – Conical Arrows)

Pink Noise		
t-Test: Two-Sample Assuming Equal Variances		
	Control	Conical Arrows
Mean	0.1884	0.1612
Variance	0.0010423	0.0002597
Observations	5	5
Pooled Variance	0.000651	
Hypothesized Mean Difference	0	
df	8	
t Stat	1.685576292	
P(T<=t) one-tail	0.065182908	
t Critical one-tail	1.859548038	
P(T<=t) two-tail	0.130365816	
t Critical two-tail	2.306004135	

Table A.12: Pink Noise Two Tail t-Test (Control – Block Arrows)

Pink Noise		
t-Test: Two-Sample Assuming Equal Variances		
	Control	Block Arrows
Mean	0.1884	0.1522
Variance	0.0010423	0.0003587
Observations	5	5
Pooled Variance	0.0007005	
Hypothesized Mean Difference	0	
df	8	
t Stat	2.162591567	
P(T<=t) one-tail	0.031268178	
t Critical one-tail	1.859548038	
P(T<=t) two-tail	0.062536355	
t Critical two-tail	2.306004135	

Appendix B: Pink Noise Frequency Spectra

NOTE: All spectra are plotted with volume in dB on the y-axis and frequency on the x-axis. Data that lies below the -60 dB threshold is considered inaudible to the human ear. All frequencies on the spectra lie within the human hearing band (20 Hz – 20 kHz).

CONTROL 1

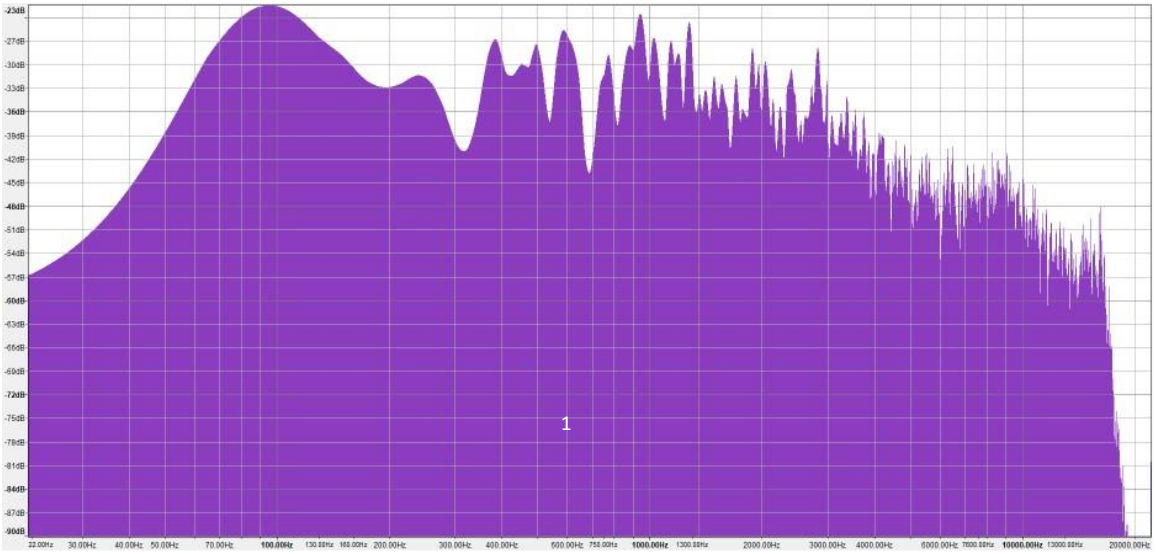

Figure B.1: Pink Noise Frequency Spectra of Trial 1 Control

CONTROL 2

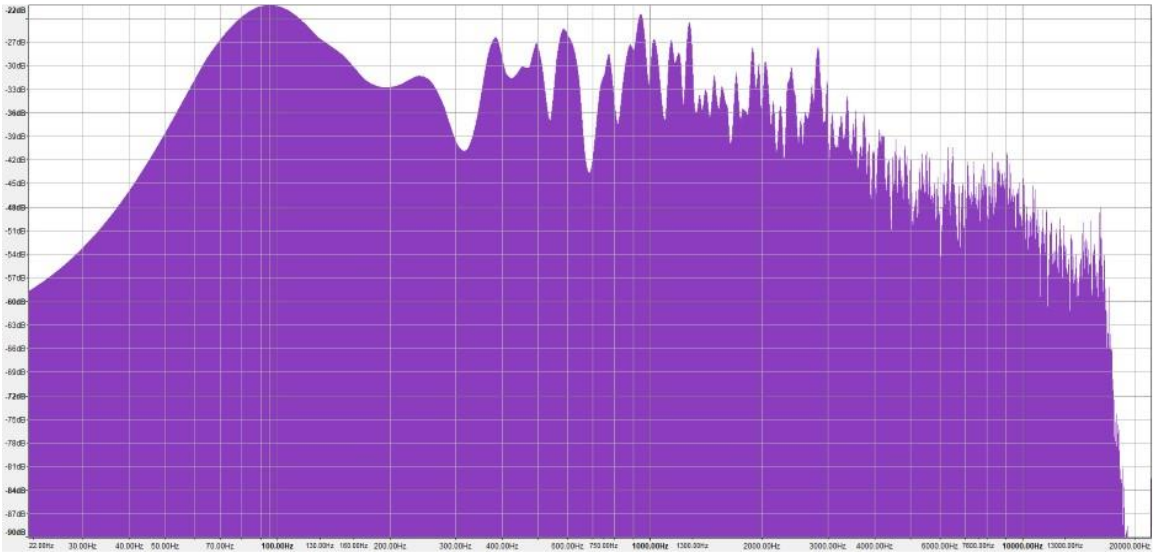

Figure B.2: Pink Noise Frequency Spectra of Trial 2 Control

CONTROL 3

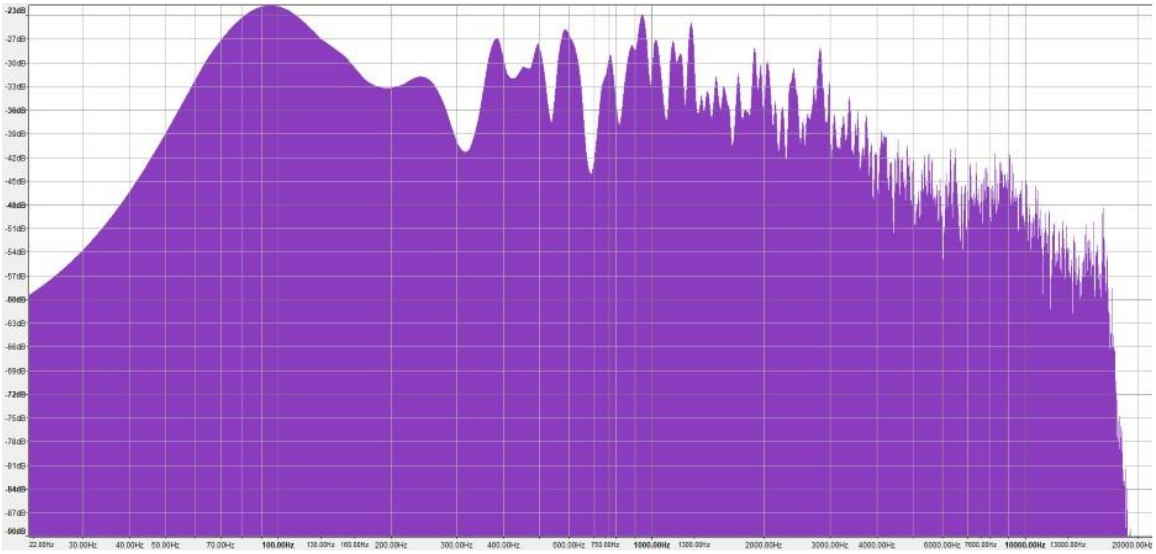

Figure B.3: Pink Noise Frequency Spectra of Trial 3 Control

CONTROL 4

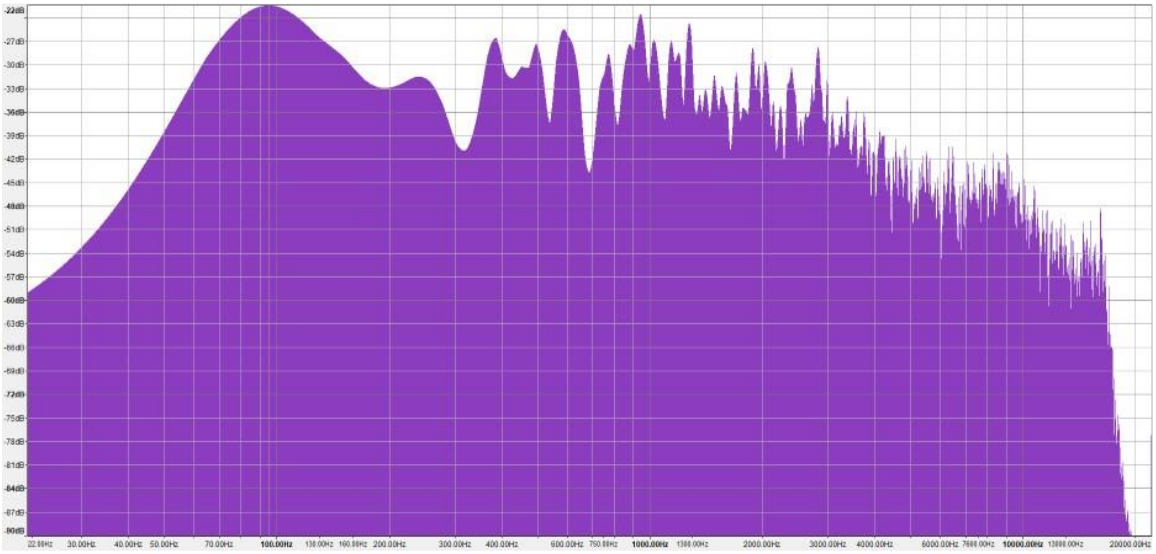

Figure B.4: Pink Noise Frequency Spectra of Trial 4 Control

CONTROL 5

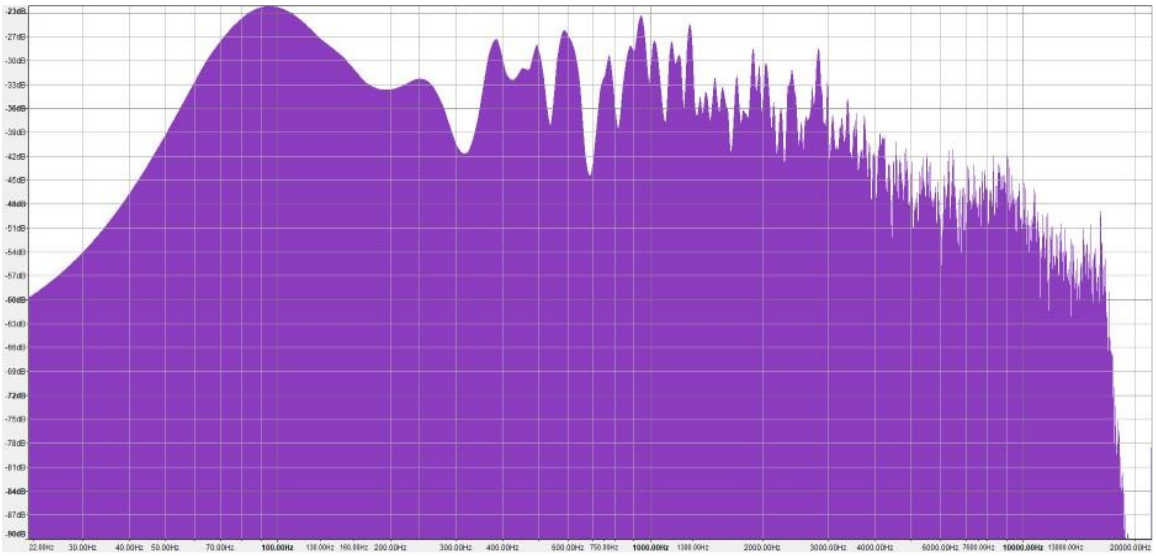

Figure B.5: Pink Noise Frequency Spectra of Trial 5 Control

Parabolic Disc 1

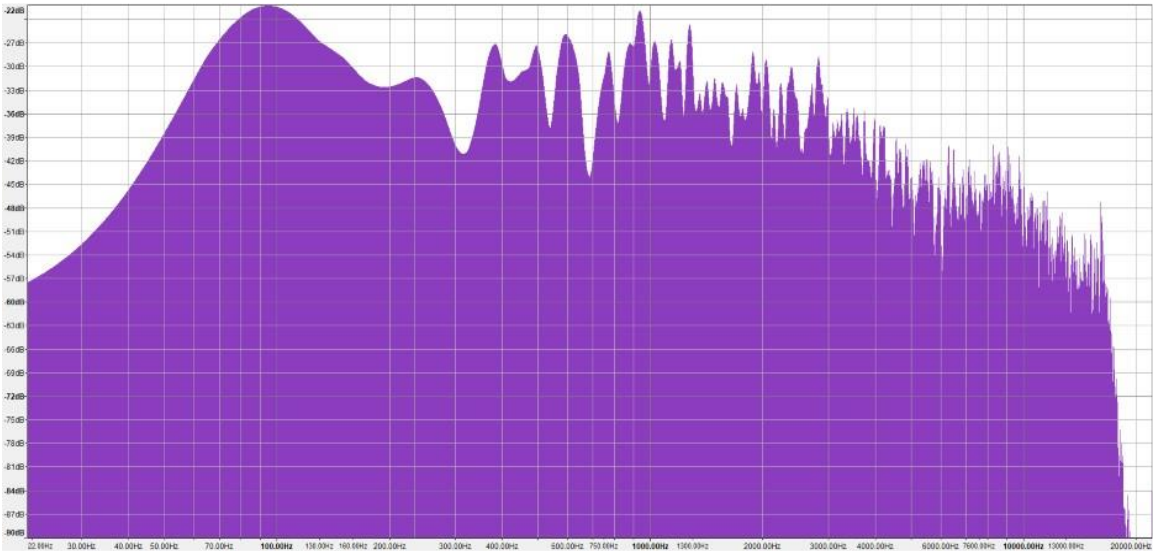

Figure B.6: Pink Noise Frequency Spectra of Trial 1 Parabolic Disc

Parabolic Disc 2

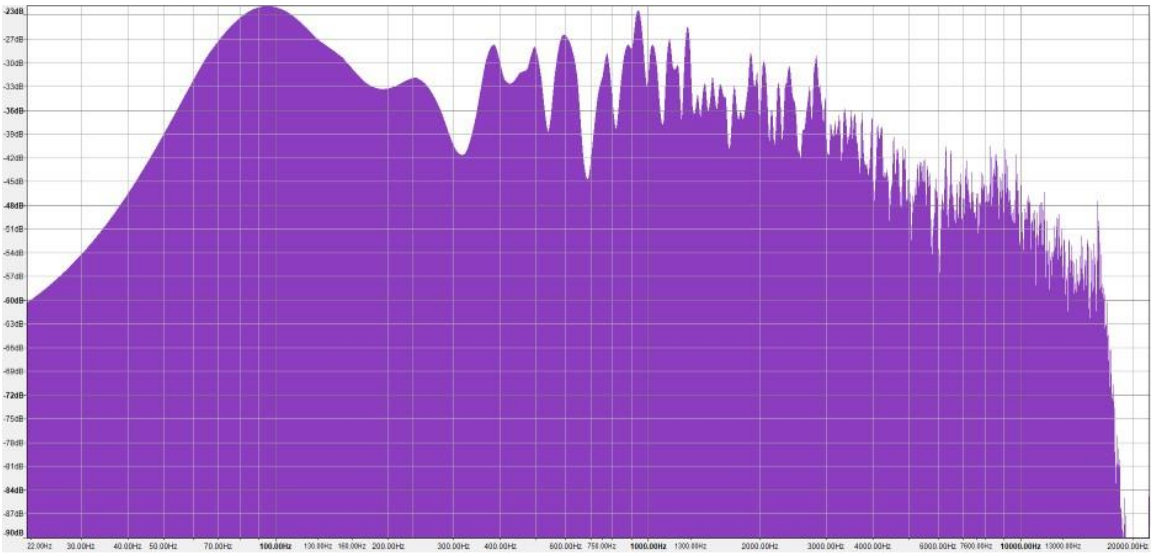

Figure B.7: Pink Noise Frequency Spectra of Trial 2 Parabolic Disc

Parabolic Disc 3

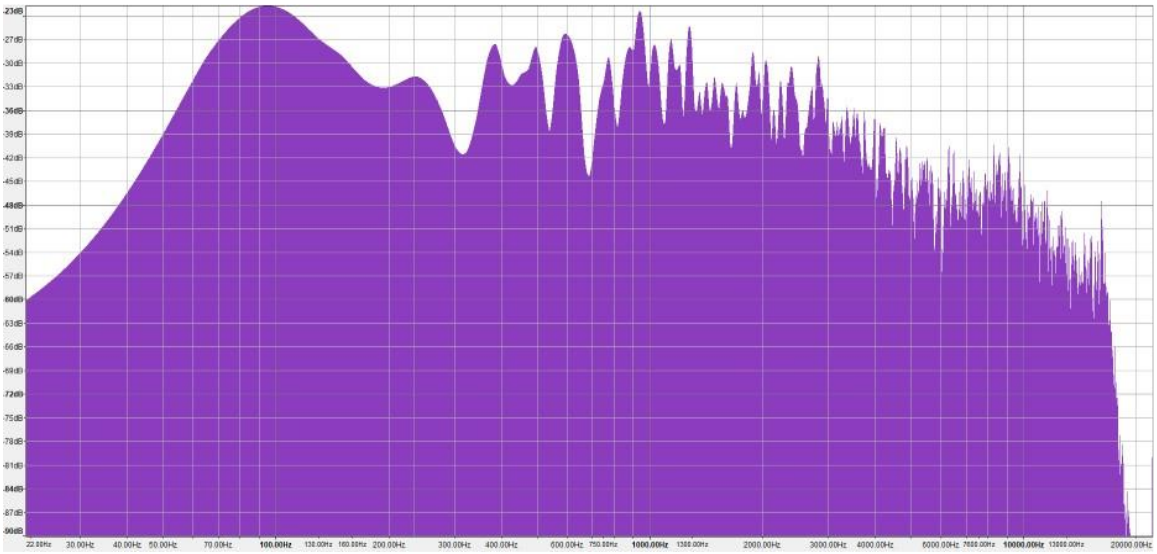

Figure B.8: Pink Noise Frequency Spectra of Trial 3 Parabolic Disc

Parabolic Disc 4

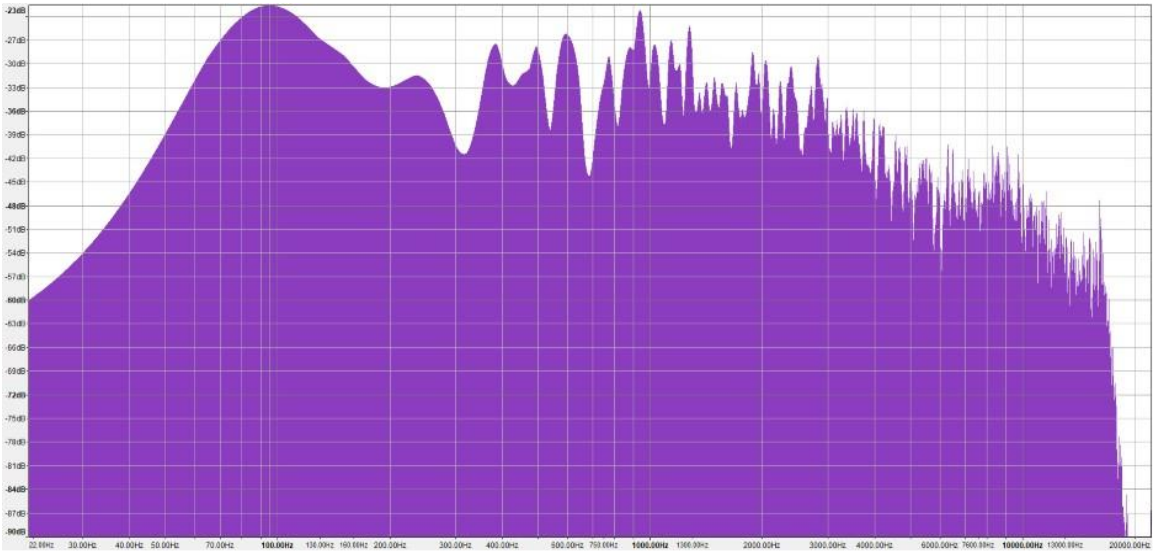

Figure B.9: Pink Noise Frequency Spectra of Trial 4 Parabolic Disc

Parabolic Disc 5

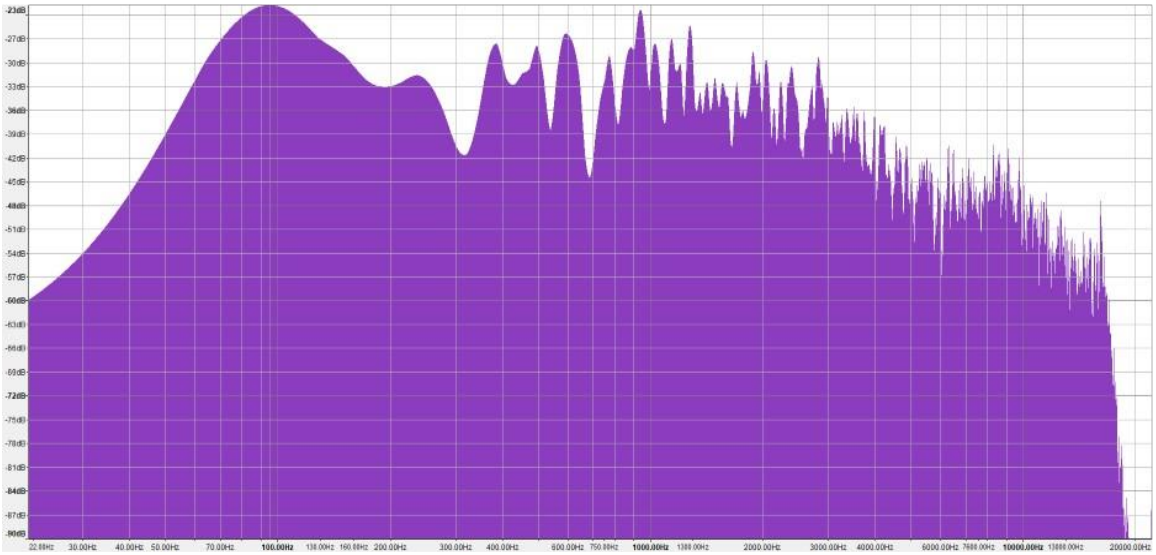

Figure B.10: Pink Noise Frequency Spectra of Trial 5 Parabolic Disc

Phononic Crystal 1

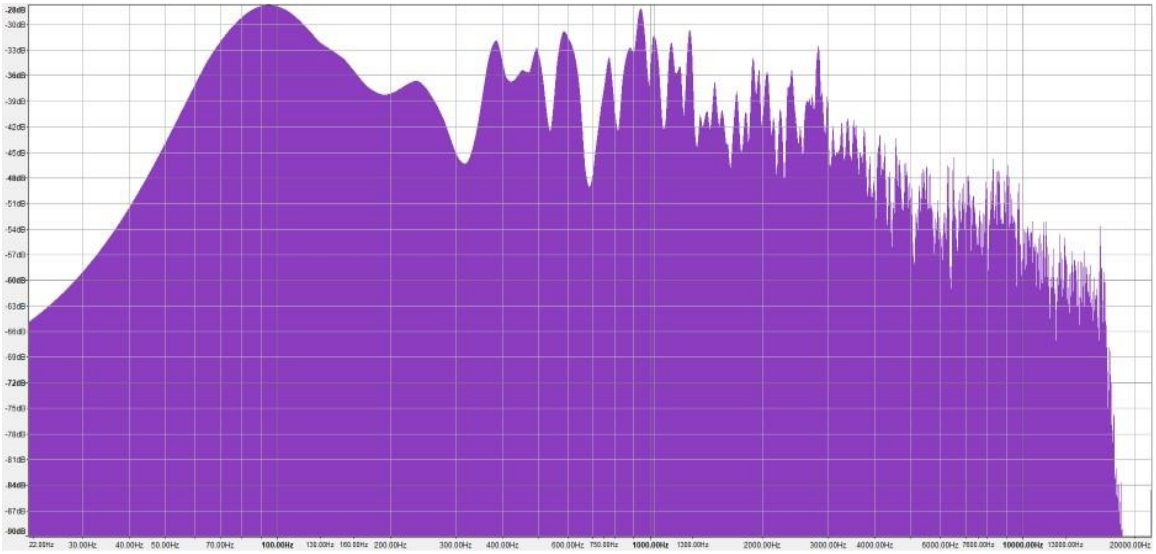

Figure B.11: Pink Noise Frequency Spectra of Trial 1 Phononic Crystal

Phononic Crystal 2

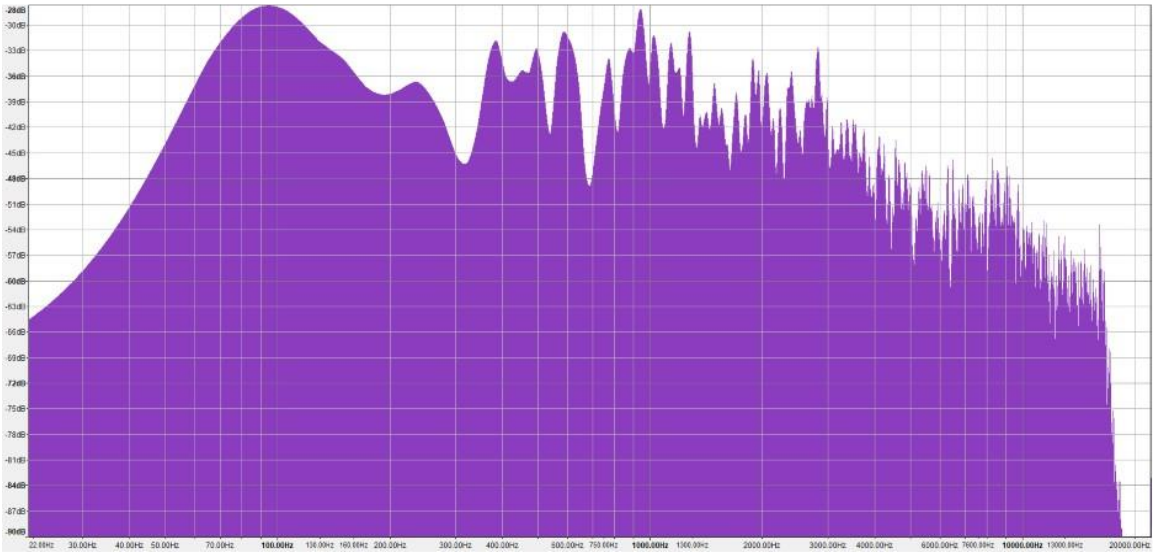

Figure B.12: Pink Noise Frequency Spectra of Trial 2 Phononic Crystal

Phononic Crystal 3

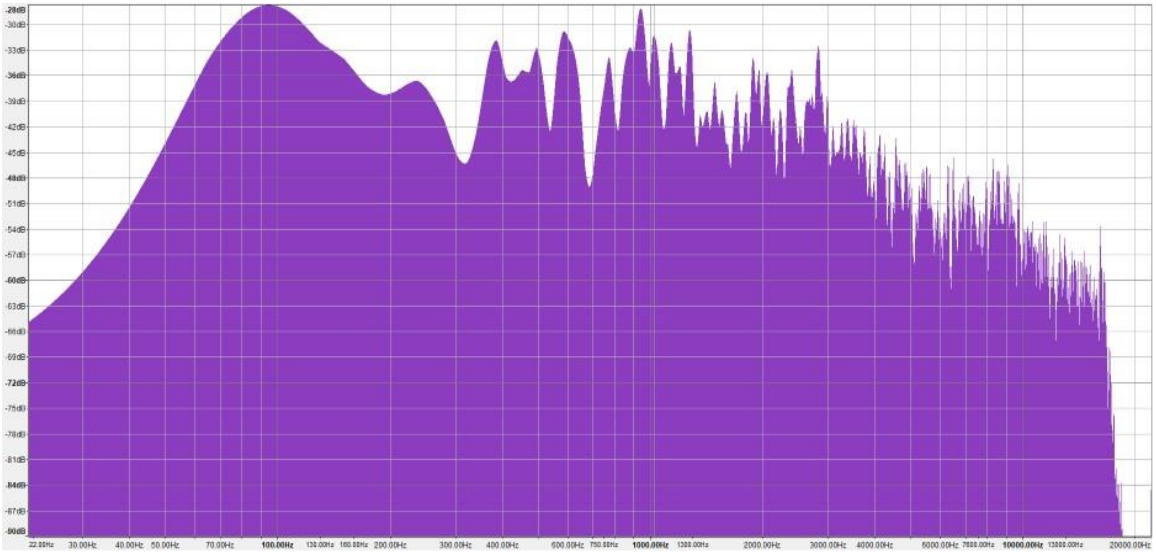

Figure B.13: Pink Noise Frequency Spectra of Trial 3 Phononic Crystal

Phononic Crystal 4

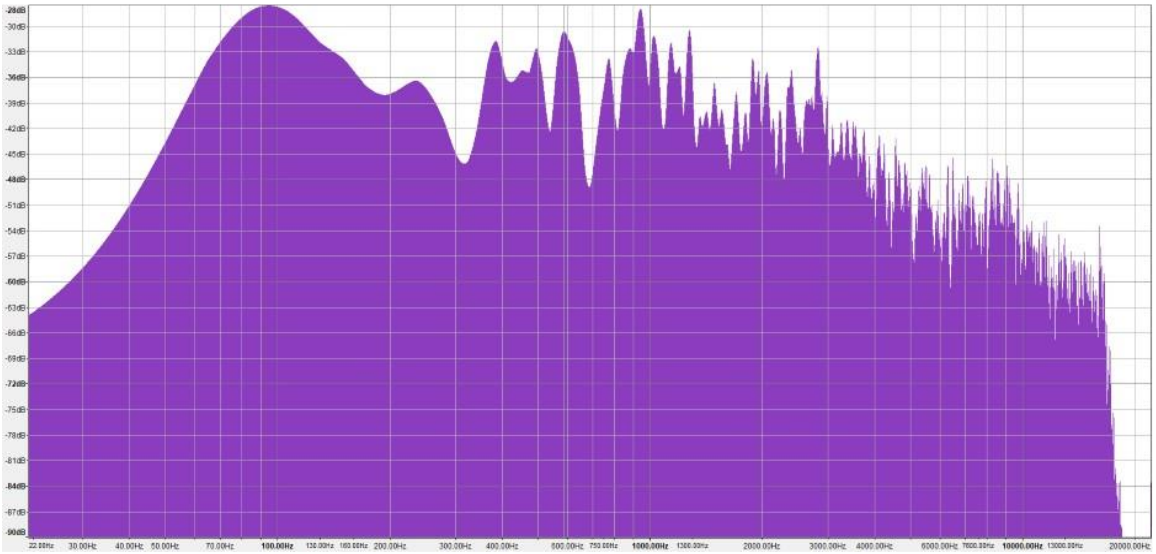

Figure B.14: Pink Noise Frequency Spectra of Trial 4 Phononic Crystal

Phononic Crystal 5

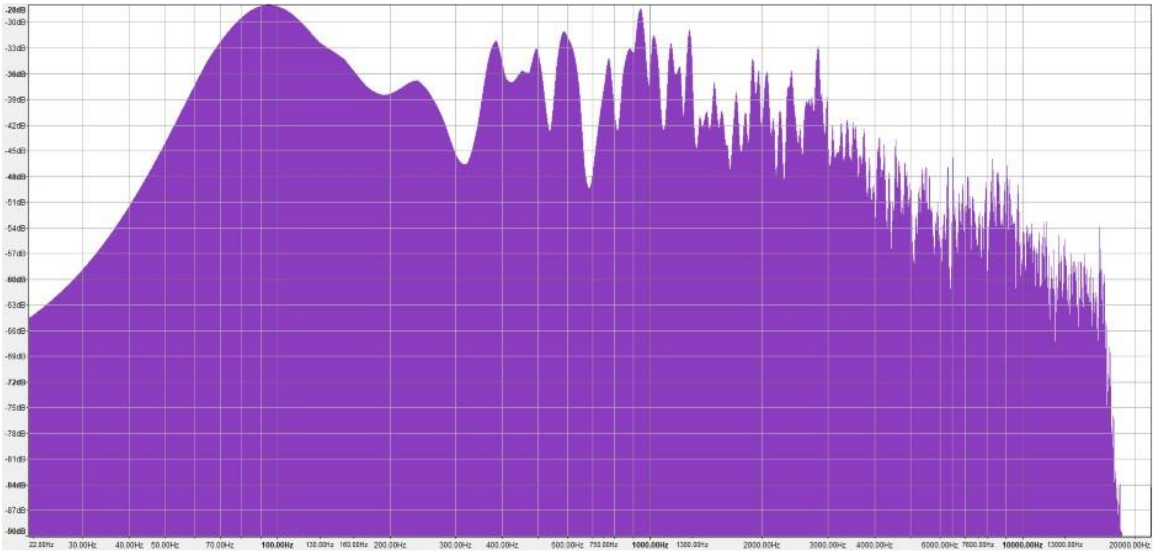

Figure B.15: Pink Noise Frequency Spectra of Trial 5 Phononic Crystal

Conical Arrows 1

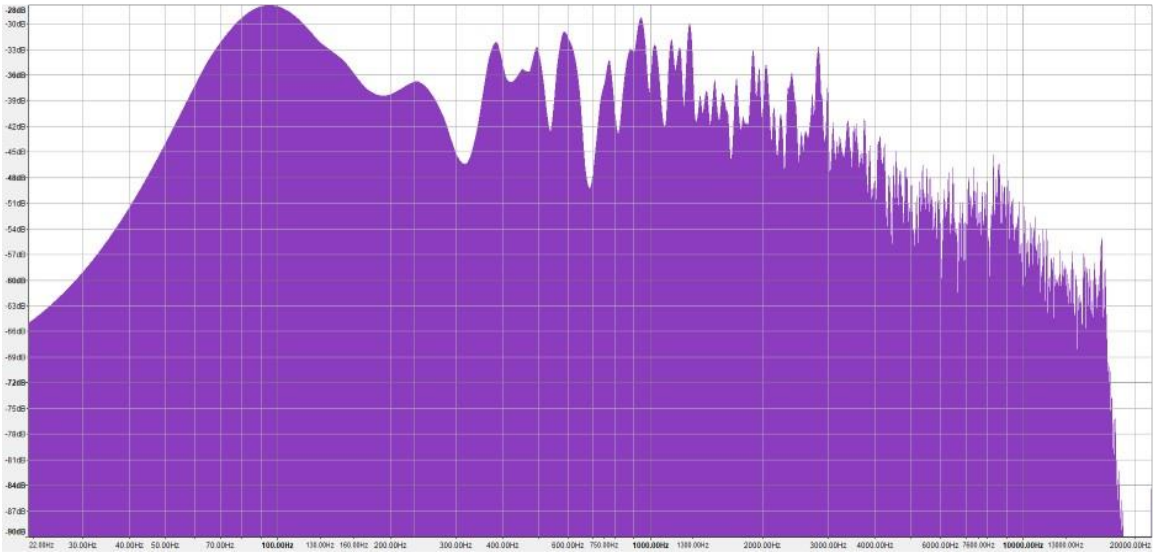

Figure B.16: Pink Noise Frequency Spectra of Trial 1 Conical Arrow

Conical Arrows 2

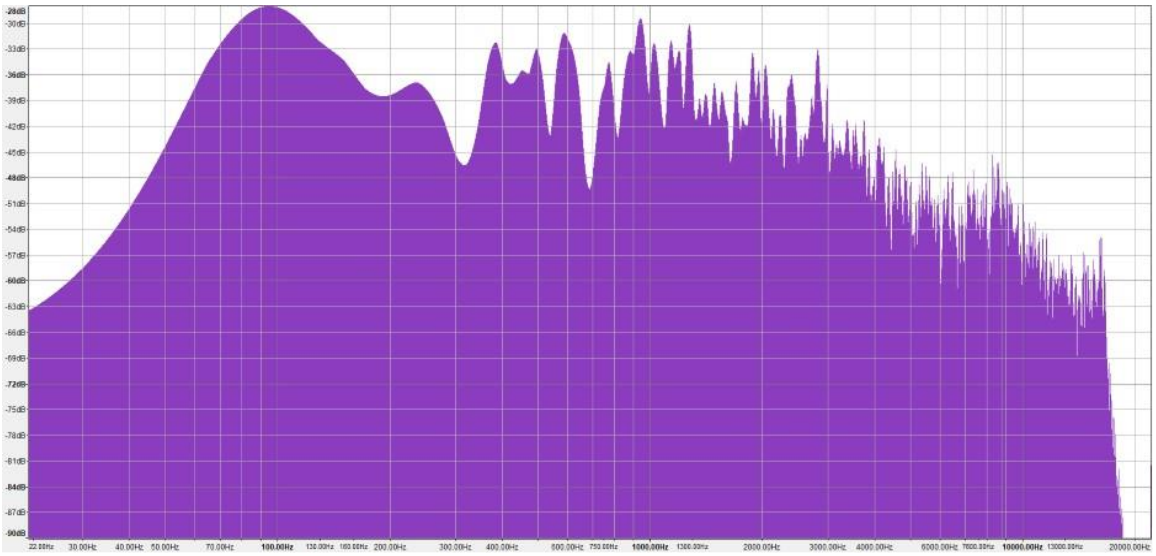

Figure B.17: Pink Noise Frequency Spectra of Trial 2 Conical Arrow

Conical Arrows 3

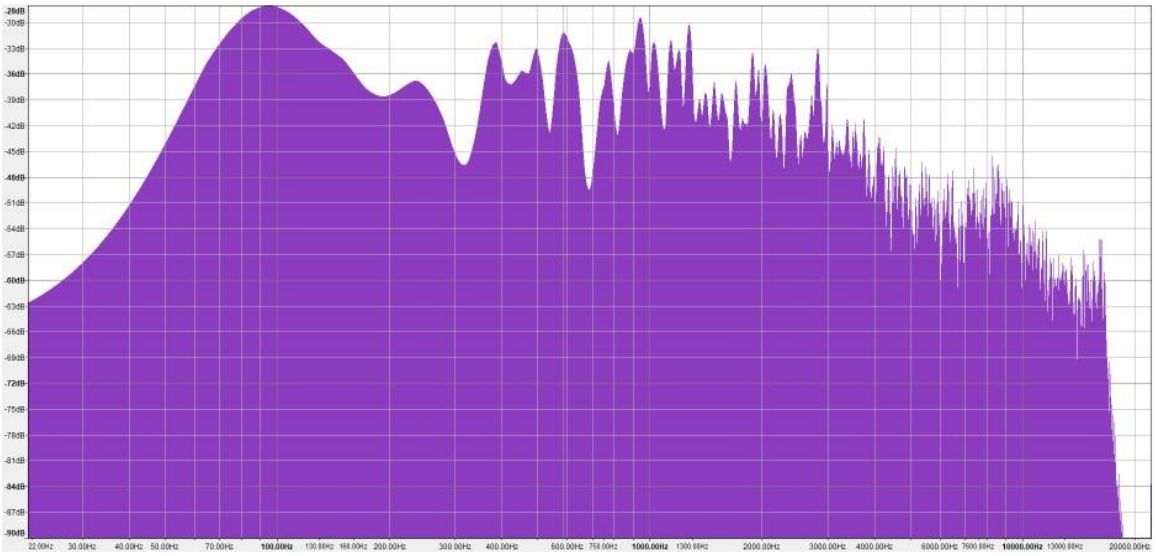

Figure B.18: Pink Noise Frequency Spectra of Trial 3 Conical Arrow

Conical Arrows 4

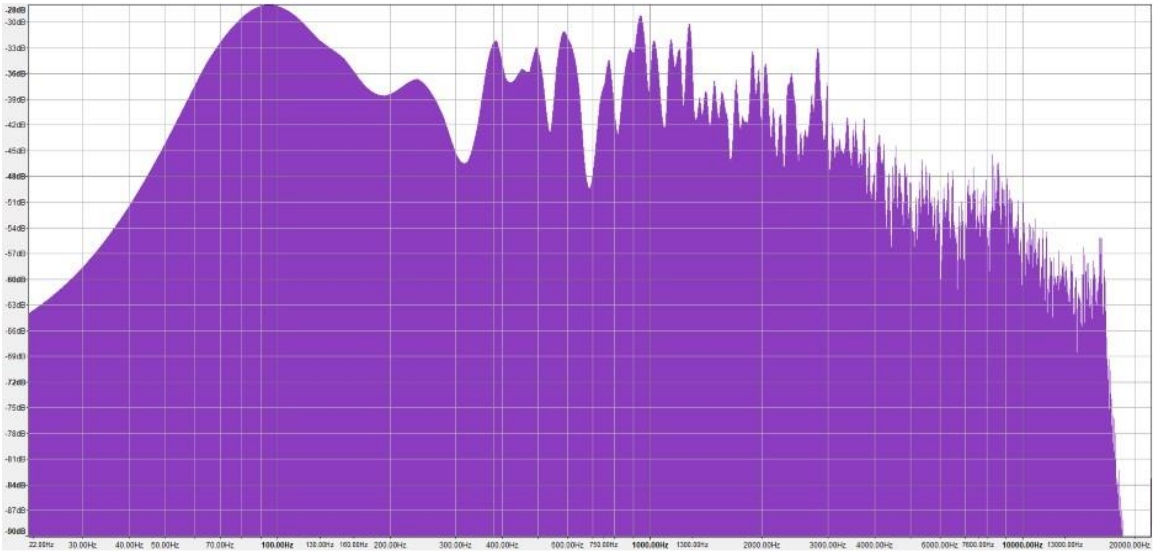

Figure B.19: Pink Noise Frequency Spectra of Trial 4 Conical Arrow

Conical Arrows 5

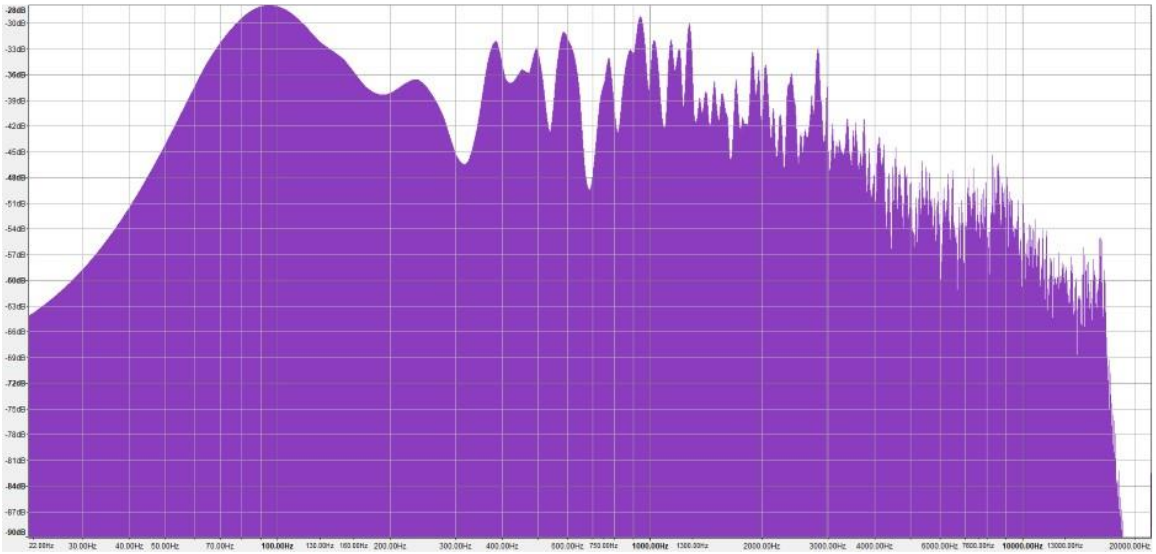

Figure B.20: Pink Noise Frequency Spectra of Trial 5 Conical Arrow

Block Arrows 1

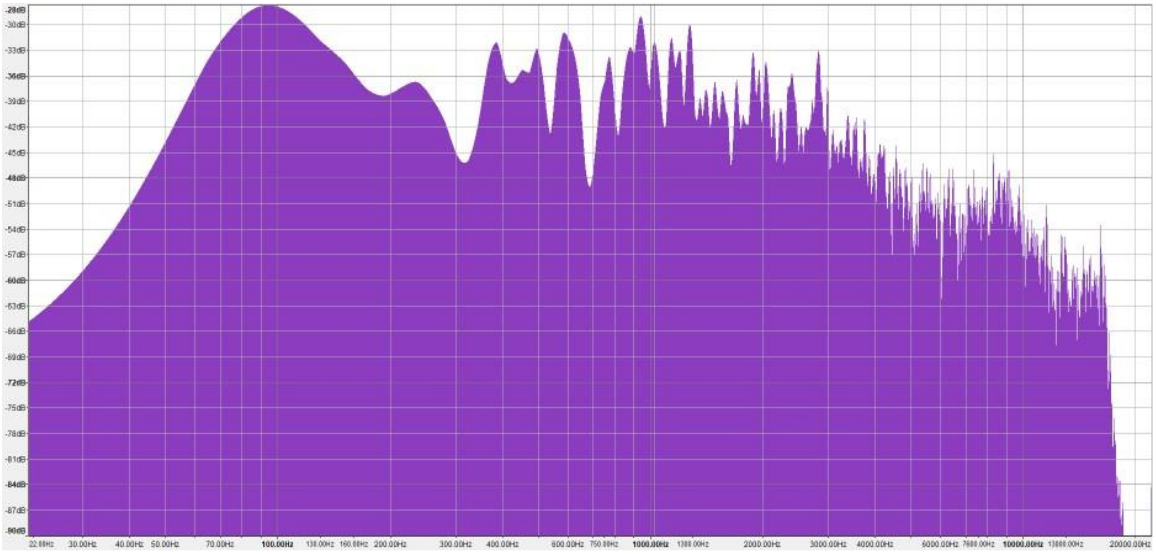

Figure B.21: Pink Noise Frequency Spectra of Trial 1 Block Arrow

Block Arrows 2

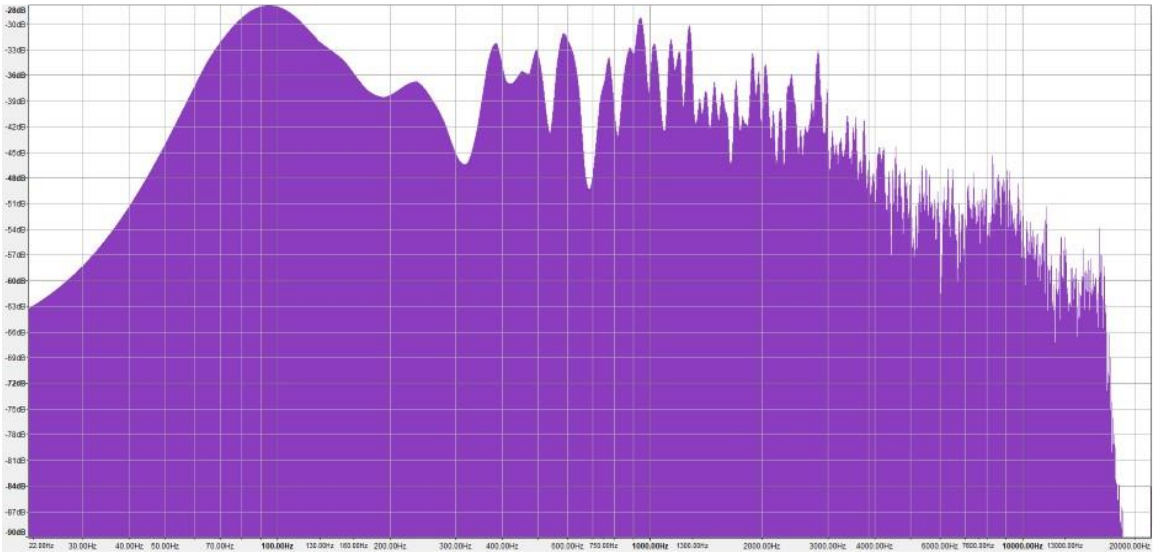

Figure B.22: Pink Noise Frequency Spectra of Trial 2 Block Arrow

Block Arrows 3

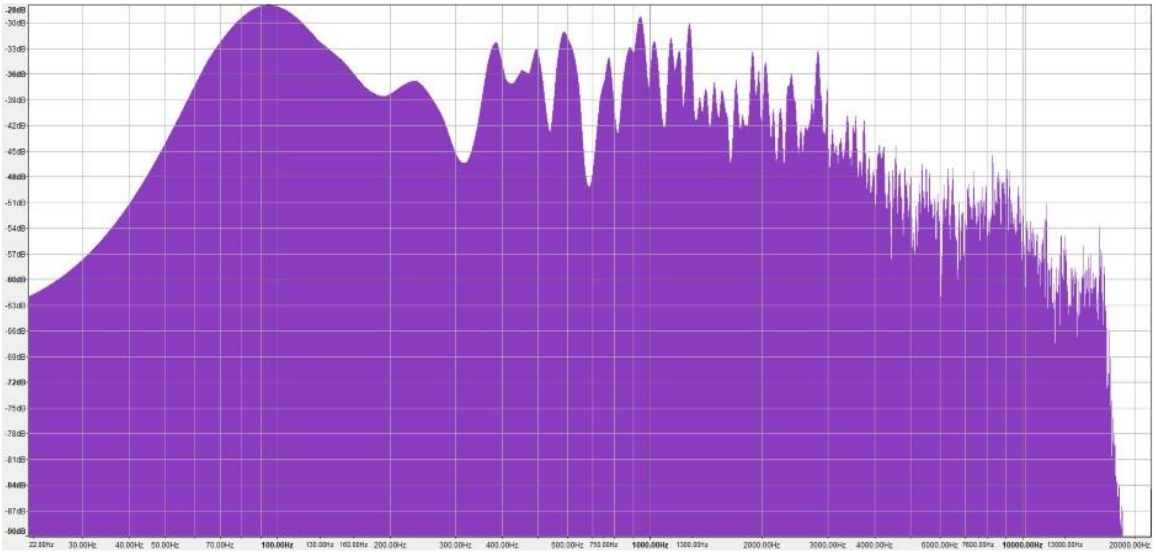

Figure B.23: Pink Noise Frequency Spectra of Trial 3 Block Arrow

Block Arrows 4

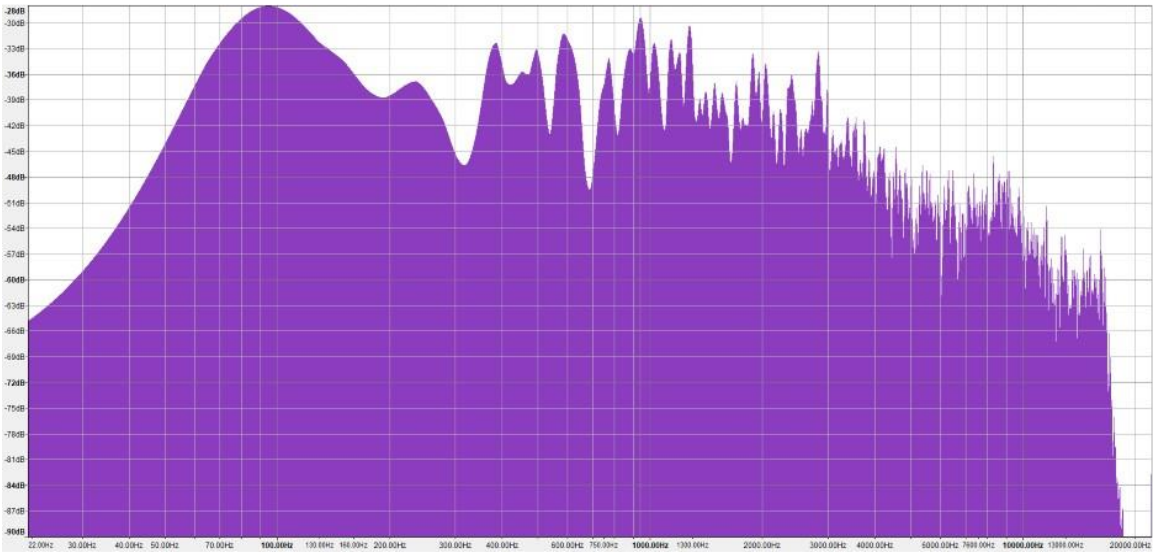

Figure B.24: Pink Noise Frequency Spectra of Trial 4 Block Arrow

Block Arrows 5

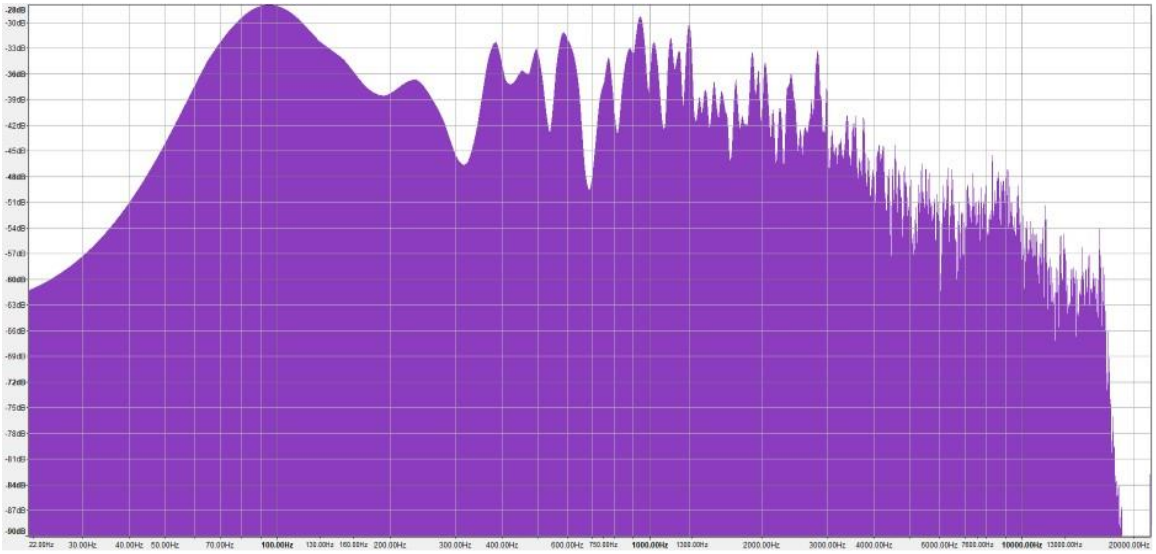

Figure B.25: Pink Noise Frequency Spectra of Trial 5 Block Arrow